Blue Stragglers in Galactic Open Clusters and the Integrated Spectral Energy Distributions

Y. Xin and L. Deng

National Astronomical Observatories, Chinese Academy of Sciences, Beijing 100012

`xinyu@bao.ac.cn, licai@bao.ac.cn`

ABSTRACT

Synthetic integrated spectral properties of the old Galactic open clusters are studies in this work, where twenty-seven Galactic open clusters of ages $\geq$ 1Gyr are selected as the working sample. Based on the photometric observations of these open clusters, synthetic integrated spectrum has been made for the stellar population of each cluster. The effects of blue straggler stars (BSSs) on the conventional simple stellar population (SSP) model are analyzed on an individual cluster base. It is shown that the BSSs, whose holding positions in the color-magnitude diagrams (CMDs) cannot be predicted by the current single-star evolution theory, present significant modifications to the integrated properties of theoretical SSP model. The synthesized integrated spectral energy distributions (ISEDs) of our sample clusters are dramatically different from the SSPs based on isochrone only. The BSSs corrected ISEDs of stellar populations show systematic enhancements towards shorter wavelength in the spectra. When measured with wide-band colors in unresolvable conditions, the age of a stellar population can be seriously under-estimated by the conventional SSP model. Therefore, considering the common existence of BSS component in real stellar populations, a considerable amount of alternations on the conventional ISEDs should be expected when applying the technique of evolutionary population synthesis (EPS) to more complicated stellar systems.

Subject headings: blue stragglers — open clusters and associations: general — Galaxy: stellar content — galaxies: stellar content

1. INTRODUCTION

By many years of substantial practice, evolutionary population synthesis (EPS) has been proved to be a powerful tool for the study of the evolution of stellar systems. EPS

method is based on the great success of the understanding of stars, including stellar structure and evolution (without taking into account rotation, magnetic field and binarity), and the properties of stellar radiation from their atmospheres. As the basic building blocks of synthetic spectra of galaxies, simple stellar populations (SSPs) are built with the integration of the library of isochrones based on the theoretical evolutionary tracks, the library of stellar spectrum of individual stars, and the stellar initial mass function (IMF). The first two ingredients are given at a certain chemical composition, while the IMF is usually considered as universal (see Bressan et al. 1994, for a review).

As the solid base for studying complex stellar systems, EPS method is very successful in many aspects. In analyzing the stellar populations of composite systems such as galaxies, EPS reproduces the overall spectral properties of the stellar components, and also derives star formation and chemical evolution history (Schulz et al. 2002). In the case of simple stellar systems such as star clusters, relying on almost perfect isochrone-fitting to the photometric observations of the systems, the conventional SSP model can give fairly good interpretations upon most of the evolutionary features of star clusters, i.e., the main sequence (MS), red giant branch (RGB), horizontal branch (HB) or red clump giants on the integrated light of these components. However, exceptions do exist. It is often observed that a certain number of definite member stars have holding positions in the color-magnitude diagrams (CMDs) that cannot be predicted by the single-star evolution theory, and consequently the integrated contributions of these stragglers to the total radiation are ignored by the conventional SSP model. Most of the unresolved objects are related to binary scenario and stellar collisional events, such as blue straggler stars (BSSs) in stellar systems. In the case of open clusters, being the most luminous blue objects, BSSs can raise a big challenge to the SSP model (Deng et al. 1999; Schiavon et al. 2004).

Since the first identification by Sandage (1953) in the cluster M3, BSSs have been observed in almost all star clusters, dwarf galaxies and presumably in all other stellar systems (Stryker 1993). These enigmatic stars locate bluer and brighter of the cluster turnoff region in a CMD, and appear *straggling* away from the regular evolutionary path, hence are named 'blue stragglers'. As for the nature of these objects, observations suggest that BSSs are more massive than the regular stars in the turnoff region, thus they are most likely the remnants of stellar merger events, or still binary systems with luminous blue components.

The primary ways of the formation of BSSs are dynamical evolution of close binaries, and collisions in the high density area in the clusters. (Ferraro et al. 1997; Piotto et al. 1999; Ferraro et al. 2003). As suggested by mounting evidence, if BSSs are partially the result of mass transfer or coalescence during resonant interactions involving binary systems (Leonard 1989; Bacon et al. 1996), they would be the visible tracers of binary populations, and addi-

tionally they provide an opportunity for learning how interactions in binary systems affect stellar evolution (Pols & Marinus 1994). Meanwhile, appreciable frequency of single-single star collisions generally occur only in the cores of the densest clusters (Hills & Day 1976), where BSSs can provide observational constraints on stellar collision cross sections for tidal captures, direct collisions, and the corresponding productions in dense stellar environment (Bailyn 1995; Lombardi et al. 2002). Regardless of the origins of BSSs, when mergers occur, many of the cluster properties are affected. Remarkable central concentration of BSSs provides an effective examination on cluster dynamics, such as two-body relaxation in binary systems, core collapse rate, mass segregation and depletion of low mass stars in stellar systems, and energy equipartition among the cluster member stars. Moreover, BSSs do exist in significant numbers in both young and old populations. They provide a remarkable hotter component with respect to the rest of the cluster (Manteiga et al. 1989) and bring on possible bluer integrated colors and integrated spectral energy distributions (ISEDs) (Deng et al. 1999). Therefore, the presence of numerous BSSs has to be accounted in population synthesis definitely for star clusters, and possibly for dwarf ellipsoidals, ellipticals and other galaxies. It is important to gather empirical information on BSSs in order to characterize correctly the overall properties of populations in stellar systems according to integrated light studies.

Based on the assumption that all members are born simultaneously therefore having the same age and metallicity, open and globular clusters are considered as the best SSP templates in the real world (Bica & Alloin 1986; Battinelli et al. 1994). In this paper, our attention is put on the BSSs in Galactic open clusters. The reason is that, for the chemical composition range covered by Galactic population I clusters, BSSs are the most luminous blue objects whose contributions to the integrated light are more prominent, and this is especially outstanding for old open clusters when the red clump instead of blue HB is populated. The BSS effects on the ISEDs become far less important for the Galactic globular clusters, where the most luminous blue objects are the HB stars.

Since the direct observation of cluster integrated light (Bica & Alloin 1986) can not attack the problems of field contamination and gravitational evaporation of low-mass stars, it is not possible to get the proper ISED of a cluster in that way. Pure theoretical efforts based on the current theory of stellar evolution also fail at this point simply due to the stragglers. Keeping these in mind, we propose a semi-empirical approach of building cluster ISED in our previous work (Deng et al 1999): after careful membership analysis, the general stellar ingredients well fitted by a theoretical isochrone is represented by the conventional SSP model, in which the 'missing' low mass stars can be recovered with proper initial mass function, so that the true meaning of SSP is conserved; and all the stragglers are included into the ISED by derivation of the spectra from observations.

The importance of BSSs on the studies of stellar formation and evolution, and population analysis of galaxies have been stressed by numerous work (see Stryker 1993 for a review). What we are going to show in this paper, by using old Galactic open clusters, is that the effects of BSSs on the integrated light of a stellar system and on the theoretical model of SSP. With a sample of twenty-seven Galactic open clusters of ages ≥ 1 Gyr, we present in this work a set of integrated spectra and modified integrated B-V color of the clusters. Comparison between the conventional approach and our results is made aimed at investigating BSSs contribution to the conventional SSP model. A short report of our working sample is given in the next section. In Section 3, population synthesis is performed for each cluster. BSSs are treated as hydrogen-burning MS stars, whose spectra are selected from Lejeune (et al. 1997,1998) stellar spectral library, given the physical quantities by fitting evolutionary tracks to their observed positions in the CMDs. The other stellar ingredients in a cluster are approximated with Padova isochrone (Bertelli et al. 1994). The final ISED of a cluster is the combination of these two components. BSSs contribution to the conventional ISEDs varies for different clusters depending on the basic quantities of the cluster and the BSS component. Discussions addressing these issues are given in Section 4. In Section 5, BSSs modification to the integrated properties of SSP model in terms of wide-band B-V color is presented, and the corresponding consequences on age determination of a SSP is also considered. The concluding remarks on our work are presented in Section 6.

2. THE WORKING SAMPLE

Photometric data of a large number of Galactic open clusters and their BSS members were published by Ahumada & Lappaset (1995, AL95 hereafter). This data set enables good access to the study of BSS population in open clusters. Due to the reasons discussed below, only twenty-seven Galactic open clusters of ages ≥ 1Gyr are selected from AL95 as our working sample. For the younger clusters, there are no clearly defined turnoff point, therefore definite BSSs identification cannot be given, and due to short lifetime and usually low member star richness, some phases in the CMD are not populated to ensure good statistics.

The basic parameters of the selected clusters are given in Table 1, where columns 1-3 give the cluster name and equatorial coordinates R.A & Dec. (2000); columns 4-7 are the ages, color excesses (E(B-V)), distance modula (DM) and metallicities (Z) of the clusters; the N_{BS} (number of BSSs) and N_2 numbers are listed in columns 8 and 9, respectively; and finally, column 10 is the reference-number. The N_{BS} numbers and BSSs photometric data for selected clusters are directly quoted from AL95. The N_2 number listed in column 9 in Table 1 is also from AL95, which is defined as the number of stars within 2 magnitudes interval below

the turnoff point for a given cluster. The other basic parameters of the selected clusters, specifically the age, Z, E(B-V) and DM, are extracted from the more recent photometric and theoretical work when results newer than AL95 are available.

N_2 is regarded as a very important parameter indicating the richness of theoretical stellar component in the simple population synthesis scheme. For each cluster, this count is made from the same CMD where the BSSs are selected. Then, the ratio of N_{BS}/N_2 can be taken as a specific BSS frequency in a cluster, and can be used as a probe for the cluster internal dynamic processes concerning BSS formation. Figure 1 is the cluster number distribution of twenty-seven sample open clusters as functions of four different parameters: Age, Z, N_{BS} and N_{BS}/N_2. There is scarcely very old clusters in our working sample. The oldest one is 8 Gyr. More than one half of the clusters are metal-poor with respect to solar abundance. The metallicity distribution peaks at less than a half solar value (Z=0.007). The cluster distributions in both N_{BS} and N_{BS}/N_2 are inclined to low numbers, which means that the clusters have neither large number of member stars nor BSSs. Only two clusters possess BSSs more than thirty. The ratio of N_{BS}/N_2 is confined in a region between 0.05 and 0.25. Figure 2 shows us the BSS numbers of our sample clusters as functions of cluster age and N_2 number, where there is no indication of any correlation between N_{BS} and cluster age (Fig. 2a), while a good correlation with N_2 is well defined (Fig. 2b).

It is worth emphasizing here that not all the clusters have complete membership determinations in terms of both proper motion and radial velocity. The selection of BSS candidates in AL95 is basically according to their appearance regions in the observed CMDs. In our work, all the BSSs are treated equally without any further detailed membership measurements and BSSs identification. Such a treatment inevitably suffers some problems which will be addressed in Section 4.

3.   THE SYNTHETIC SED OF THE CLUSTER

An ideal SSP model could be applied to an open cluster in terms of metallicity and age of its members, if all stars in it were single (at least not interactive binaries), and the low-mass members were conserved against the tidal effects. Unfortunately, the nature turns us down at this point. The obvious differences between a SSP and a real star cluster should be the stars resulted from interacting binaries, stellar collisions and evaporation of the low mass components. In old open clusters, since RGB stars and red clump giants have been well populated, the red stragglers can hardly alter the integrated light of a SSP due to their rare numbers and low luminosities compared with RGB and the clump giants within the same cluster. Therefore, the most prominent features in the CMDs in open clusters are the

luminous BSSs.

According to above discussions, the stellar population of a cluster is assumed to be composed of two components in our work. The first one is a package of all the member stars fitted by an isochrone in the CMD, plus the low-mass stars that have been peeled off by tidal effects. This is obviously nothing but the conventional SSP model and named as the SSP component for use in the following text. The second one includes all the other members straggling away from the isochrone. In the light of above discussions, only BSSs are considered into this component. We label it as the BSS component.

Assuming that the cluster CMD can be well fitted by a theoretical model, the SSP component of a cluster can be substituted with a theoretical isochrone that best fits the age and metallicity of the cluster. While, the BSS component is specified in the CMD with photometric data of AL95. Figure 3 shows the composite CMD of NGC 6791 as an example, where the solid line is the isochrone, the dotted line is the zero age main sequence (ZAMS), and the dots are the BSSs defined by photometry. We notice that there is a number of objects located below the ZAMS loci. This is partly due to observational uncertainties.

3.1. Getting the theoretical spectra of the BSSs

It is a growing consensus that the major mechanisms of BSS production are mass-transfer and merger events in close binary systems, or stellar collisions in dense environment (Schönberner & Napiwotzki 1994). The physically interactive processes in binary systems will transfer fresh hydrogen fuel from hydrogen-rich envelop to hydrogen-depleted or ex-hausted core and re-ignite it, which makes the remnants behave like MS stars (Benz & Hills 1987,1992), as such, BSSs are treated as hydrogen-burning MS stars in our work. Their masses, luminosities and effective temperatures can be determined by fitting their positions in the CMD with evolutionary tracks of higher masses than the turnoff. Given the effective temperature (T_{eff}) and surface gravity ($log\ g$), a theoretical spectrum from the library (Lejeune et al. 1997,1998) can be assigned to the BSSs. This process is performed for all the BSSs in our sample clusters.

As shown in Figure 3, there are some BSSs located below the ZAMS. Except for possible photometric errors, their missing-positions are most likely due to the helium-enrichment in the atmosphere after merger events (Benz & Hills 1987,1992). The intrinsic properties of these stars need more carefully observational studies. In our work, these low-luminosity BSSs are not considered in computing the ISEDs of the clusters, since their contributions to the integrated light are even much lower than the stars in the turnoff region.

3.2. Getting the ISED of a cluster

The purpose of our work is to build modified ISEDs based on the observations of open clusters, so the clusters as a whole will be treated as unresolvable stellar populations. Most of the cluster member stars can be in principle confined in the single-star evolution regime, including the unresolved binaries shown in photometric binary sequence in the CMDs. As the SSP component is based on single-star evolution theory, we should emphasize here that the IMF applied to conventional SSP model should account for both the single stars and the photometric binary stars in the observational CMDs. For a given cluster of age t and metallicity Z, assuming Salpeter IMF $\phi(m)$, the ISED of SSP component is,

$$F_{iso}(\lambda, t, Z) = A \int_{m_l}^{m_u} \phi(m) f(\lambda, m, t, Z) dm \tag{1}$$

where $f(\lambda, m, t, Z)$ is the flux of a star of mass m, age t and metallicity Z. A is a normalization constant which is fixed by the cluster richness parameter N_2. m_u and m_l are the upper and lower integration limits, in the current context, m_u is the initial mass of the most massive living star at the age of the cluster, while m_l takes its regular meaning.

By using Salpeter IMF, A is derived from the formula:

$$N = A \int_{m_1}^{m_2} m^{-2.35} dm = N_2 \tag{2}$$

where m_1 and m_2 are the initial masses corresponding to the two limiting magnitudes defined by N_2, i.e. m_2 is the initial mass of the very star in the turnoff, and m_1 is the initial mass of star whose magnitude is two magnitudes lower than that of the cluster turnoff point.

For the BSS component, the integrated spectra $F_{BS}(\lambda, t, Z)$ is given by directly summing up the individual spectrum,

$$F_{BS}(\lambda, t, Z) = \sum_{i=1}^{N_{BS}} f_{BS}^i \tag{3}$$

where f_{BS}^i is the theoretical spectrum for a BSS, the index i runs from 1 to N_{BS}. N_{BS} is the total number of BSSs in a cluster.

Finally, the ISED of a cluster in our work is the combination of the integrated spectrum of SSP component $F_{iso}(\lambda, t, Z)$ and that of BSS component $F_{BS}(\lambda, t, Z)$.

4. BSS MODIFICATION TO THE CONVENTIONAL ISED

As discussed in above text, there are several channels of BSSs formation. Depending on the specific dynamical environment of the host clusters, and the correlation with the

richness of the cluster (see Fig. 2b), BSS population in different clusters actually presents very different properties. Therefore, BSSs effects on the final ISEDs also vary greatly among the clusters in our sample.

To demonstrate the effects of BSSs on the conventional ISEDs in the case of open clusters, Figure 4 is given with the fluxes of different ingredients, where the abscissa is the wavelength in angstrom, the integrated spectrum of the BSS component in dotted line, that of SSP component in dash line, and the total ISED (combination of the SSP and BSS components) is in solid line. In our work, the BSS modifications to the conventional SSP model can be divided into three cases: Normal star dominates (Fig. 4a), BSSs important (Fig. 4b) and BSS dominates (Fig. 4c). Regardless of the specific cases, the existence of BSS population modifies all the integrated light of our sample clusters at some extent, and these alternations are inclined towards UV and blue bands, therefore turns the spectra hotter. For different cases, the BSS population possesses certain properties, i.e., locations in the cluster, membership measurements and number richness, which are all important in interpreting the strength of BSS effects on the final ISEDs. These situations are discussed separately below.

4.1. The normal star dominate case

In our work, six of the total twenty-seven sample clusters, namely Berkeley 19, NGC 752, NGC 2243, NGC 2420, NGC 2506 and NGC 6208, are classified as this category. In this case, BSSs generally locate near the cluster turnoff point in the CMDs, and N_{BS} is a minority when compared with the turnoff region stars, so that they can not produce obvious contribution to the integrated light of the cluster (Fig. 4a). Based on the physical parameters and photometric data of sample clusters and BSSs in different work, specifications of the clusters are given below.

4.1.1. NGC 6208

The membership probabilities of the five BSSs (as in AL95) in NGC 6208 have been an ambiguous issue. Three of the five BSSs were classified as B stars and non-members by Lindoff (1972). The other two high probability member BSSs possess very low luminosities and locate below the ZAMS in the composite CMD. According to above discussion, these two BSSs can be ignored when building the ISED. After excluding the non-member BSSs, the ISED of this cluster virtually suffers no BSS correction and a conventional SSP model is retained. In Figure 5, the solid triangles are the five BSSs in NGC 6208. Ones with open

boxes are the non-member BSSs in Lindoff (1972).

These two clusters, NGC 2420 (l=198.1°, b=+19.6°) and NGC 2506 (l=230.6°, b=+9.9°), have very similar physical parameters, the richnesses defined by N_2 for them are pretty close: 140 for NGC 2420 and 130 for NGC 2506. Although both have N_{BS} numbers of twelve, the properties of BSS populations are quite different. In AL95, the BSSs data of NGC 2420 were selected from the photometric work of West (1967), covering a sky region of 7.5 arcmin around the cluster center. Four BSSs were classified as field stars in that work. In contrast to that, all the BSSs in NGC 2506 (McClure et al. 1981) have membership probabilities p $\geq$ 90%, based on the proper motion study in Chiu & van Altena (1981).

Figure 6 shows a comparison of BSSs distribution and ISED modification in these two clusters. In the CMD in left panel, the solid circles are BSSs in NGC 2506, solid triangles are BSSs in NGC 2420, and solid-line isochrone represents general stellar components in two clusters, according to their similar age (3.4 Gyr) and metallicity (Z=0.007). Although the BSS population in NGC 2420 is generally brighter than that in NGC 2506, the larger N_2 number balances this difference and makes the final ISED of NGC 2420 similar to that of NGC 2506, as shown in the right panel in Figure 6.

4.2. The BSSs important case

Over one half of our sample clusters (Berkeley 32, Berkeley 39, Berkeley 42, IC 4651, King 2, King 11, Melotte 66, NGC 188, NGC 1193, NGC 2112, NGC 2660, NGC 2682, NGC 3680, NGC 6791, NGC 6819, NGC 6939, NGC 7142 and NGC 7789) belong to the second case: BSS component seriously modifies the cluster ISED (see Fig. 4b). This situation generally happens when: (a). there is a large number of bright BSSs in the cluster; and/or (b). The N_{BS} is small, but there is a few (sometimes even just 1!) BSSs which are much brighter than the cluster turnoff point; and/or (c). the cluster is too much under-populated.

As mentioned in above context, BSSs contribution directly depends on the selection of these bright stars. More clear identification from high-definite photometric work certainly favors more accurate results. Metallicity is also a sensitive parameter to the BSSs contribution: low-metallicity ISED obviously presents stronger flux at shorter wavelength when compared with high-metallicity ISED (Schulz et al. 2002). Discussions about these problems in some sample clusters in this case are present in the following.

4.2.1. King 2

Thirty stars were cited as BSSs in King 2 in AL95, based on the Johnson-Cousins UBVR CCD photometry of Aparicio et al. (1990), in which only BSS candidates within the core radius are considered, in order to avoid the probable contamination by field stars. As a cluster of large N_{BS} number (as shown in Figure 7), the effects of BSSs on the ISED of this cluster are obviously due to the large number of bright BSSs.

4.2.2. NGC 6939

As shown in Figure 8, four stars were defined as BSSs in NGC 6939 in Cannon & Lloyd (1969). Star 59 ('59' is the identification number of the star marked in the finding chart in the photometric work of Geisler (1988). All the numbers in the following are the same identifications) was mentioned as a BSS in Geisler (1988), although it was unlikely a member. In AL95, NGC 6939 has N_2 number of eighty which is smaller than that of King 2 and bigger than that of NGC3680, thus NGC 6939 has an intermediate richness in our working sample. In this situation, the effects of BSSs on the ISED should be better attributed to the high luminosities of the BSSs, since the N_{BS} of this cluster is much smaller than that of King 2.

4.2.3. Berkeley 42 and NGC 3680

These two clusters possess small numbers of both N_{BS} and N_2. The single BSS in Berkeley 42 was selected from the CCD photometry of Aparicio et al. (1991). Four stars (29, 33, 43 and 56) were identified as BSSs in NGC 3680 in AL95, according to the photo-electric observations of Eggen (1969), who later (Eggen 1983) identified stars 3, 29, 33 and 56 as BSSs and stars 20 and 34 as 'red stragglers' with ubvy photometry. In the CCD photometry of Anthony-Twarog et al. (1991), stars 29 and 33 were considered as probable cluster members, but star 56 is unlikely a member. Meanwhile, an important presence of binaries around the turnoff point of NGC 3680 was observed by Anthony-Twarog et al. (1991). As shown in Figure 9, there is a BSS in both two clusters whose positions in the CMDs highly exceed the cluster turnoff that contributes most of the light in the blue part of the ISED.

4.2.4. Melotte 66

Melotte 66 holds a really special position in our work. Whether it should be included in this case or not is still not certain. Based on the photoelectric and photographic photometry in Hawarden (1976), the BSSs in Melotte 66 were selected in the cluster central region of 7 arcmin. However, the BSSs ISED plotted as dotted line in Figure 10 is not at all bluer than the conventional SSP spectrum, therefore the B-V color of the cluster is not modified (shown in Table 2), even though it has the largest N_{BS} of forty-six among all the sample clusters.

Furthermore, we find that forty BSSs of the cluster have rather red spectra instead of blue ones compared with the turnoff. The remaining six blue-spectrum BSSs are all located in Ring I of 3 arcmin (Hawarden 1976). In Figure 11, solid circles are the blue-spectrum BSSs. The solid rectangles are red-spectrum BSSs which should be better classified as 'yellow stragglers'. This complicated situation can be partially attributed to the significant metallicity dispersion in and around the turnoff region of the cluster (Twarog & Anthony-Twarog 1995), apart from the membership and observational uncertainty issues.

4.2.5. NGC 188

As one of the most studied old open clusters, NGC 188 has been the subject of numerous studies in many aspects, certainly including its BSS population. All the twenty BSSs in AL95 were selected from Ring I and II in the finding chart of Sandage (1962), with membership probabilities p ≥ 80% (Dinescu et al. 1996). This BSS number almost doubles the number of eleven from an earlier work of Eggen & Sandage (1969). All the BSSs show obvious high central concentration.

In the work of Dinescu et al. (1996), nine out of eleven of the BSSs in Eggen & Sandage (1969) were confirmed as cluster members with high probabilities, while the other two (D and I-102 in Sandage 1962) were excluded due to their 0% proper motion membership probabilities. Dinescu (et al. 1996) selected eleven probable BSSs with $P_\mu \geq 50\%$ and $P_{\mu,r} \geq 70\%$ ($P_{\mu,r}$ is proper motion membership probability, and $P_{\mu,r}$ is the combined probabilities of both proper motion and spatial distribution), which include five of Eggen & Sandage (1969) while adding six new BSSs. Among the six new BSSs, four are out of Ring-III and the other two are in Ring-II of Sandage (1962). Although being the latest observation of the cluster, Dinescu's BSS catalog does not show central concentration significantly higher than RGBs, therefore the original AL95 catalog is still adopted in our work.

The BSS population in this cluster has been followed intensively in the past. Although a few of BSSs are subject to dispute on their membership probabilities, the overall BSS

population still forms a considerable amount of modification to the total ISED of the cluster. This correction to the corresponding SSP model at the age and metallicity of NGC 188 is very convincing based on so much both theoretical and observational efforts.

4.2.6. NGC 2682

Similar to NGC 188, NGC 2682 (M67) has also been regarded as a classical old open cluster due to so much research work on almost all the subjects in stellar physics. The photometric data of its BSSs in AL95 was from Sanders (1989) who derived the membership measurements for the cluster stars at a earlier time (Sanders 1977). Among the total thirty BSSs in AL95, twenty-two were confirmed and two more were added by Deng et al.(1999), based on the photometric data of Beijing-Arizona-Taipei-Connecticut (BATC) sky survey and membership data from Girard et al. (1989). Figure 12 is given here to compare the possible discrimination between these two groups of BSSs identification. In the CMD (left panel), the solid dots are BSSs in AL95, open rectangles are BSSs defined by Deng et al. (1999). As shown in right panel, there is no obvious difference in the ISEDs of these two BSSs identification. The result confirms our previous work of BSSs modification to the SSP model in this cluster (Deng et al. 1999).

4.3.   The BSSs dominate case

For the third case (Tombaugh 1, NGC 1252 and NGC 2158), there is at least one extremely luminous BSS in the cluster and/or the cluster is extremely under-populated. The BSS(s) is so bright that controls almost all the integrated light of the cluster (Fig. 4c). The situation in this case raises issues such as membership probability of the bright star, and the property of such star if it is a member, just as the luminous BSS F81 in NGC 2682 (Deng et al 1999).

4.3.1. Tombaugh 1 and NGC 1252

AL95 gives only one BSS for Tombaugh 1 (Turner 1983). It appears that the cluster is a faint system that is merely visible from the field background. Turner (1983) obtained photoelectric photometry for only twenty-six stars in the cluster region. In the finding chart of Turner (1983), the BSS locates leaning on but outside the Ring I of a radius of 5 arcmin. In the CMD of Tombaugh 1 (left panel in Figure 13), it lies more than one magnitude

higher of the cluster turnoff point. In the ISED (right panel in Figure 13), this single BSS contributes about 70% of the total ISED. Especially in the wavelength shorter than 3000 $\mathring{A}$, it provides almost all the integrated light of the cluster. In this instance, the BSS is not much brighter than the turnoff, the overwhelming effect of the BSS is completely due to the under-abundant cluster members. Meanwhile, a B9.5 V star is identified as the only confirmed member BSS in NGC 1252, based on the photometric study by Bouchet & The (1983). It suffers the same problem as that on Tombaugh 1 on having very small numbers of both N_{BS} and N_2 (see Table 1). We argue that in this case, more detailed photometric work and membership measurements are inevitably needed for BSSs identification. For the moment, the ISED derived in this case is considered as direct superficial exercise, whose implication on the conventional SSP model corresponding to the age and metallicity of the cluster has little statistical significance.

4.3.2. NGC 2158

Based on the photo-electric photometry of Arp & Cuffey (1962), thirty stars were cited as BSSs in NGC 2158 in AL95. Among them, twenty-two are located in the central region of the cluster (Ring I and II), while the other eight scattered in Ring III and IV. Four BSSs were confirmed as double stars by Arp & Cuffey (1962), including the brightest BSS of the cluster (locate in Ring II), which is marked as 'D1' in Figure 14. D1 is more than 4 magnitudes brighter than the cluster turnoff point. This magnitude gap exceeds the maximum limit for BSS predicted by the mass transfer theory (McCrea 1964), just like F81 for M67 (Wheeler 1979). A new model is needed to interpret such a BSS location in the CMD, if such a star is a real member of the cluster.

To show the relative alternation of these bright stars to the conventional SSP model, Figure 15 is given here to show the flux of BSSs in different combinations in NGC 2158. The thick solid line is conventional ISED corresponding to the isochrone only. The other four lines are respectively different BSSs combinations: the long dash line is the isochrone plus all BSSs except D1; the short dash line is the spectrum of D1 alone; the dotted line is for all BSSs contribution; and the thin solid line is isochrone plus all BSSs. As shown in Figure 15, D1 dominates the ISED from UV to near IR wavelengths. It contributes almost all the energy at the spectrum shorter than 1500 $\mathring{A}$, about 80% of the integrated light of all BSSs until 4000 $\mathring{A}$, and still around 50% up to 7000 $\mathring{A}$ and beyond.

5.   Modifications to ISED in terms of wide-band B-V color

Though the effects of BSSs on SSPs' ISEDs have been clearly demonstrated by the spectral alternations of composite clusters, wide-band color is in practice more frequently used when trying to understand unresolved stellar populations in galaxies. Compared with the conventional SSP model, BSS turns the spectrum bluer. The photometric bluer color in nature corresponds to the younger stellar populations, in other words, the age will be underestimated when fitting the color with conventional SSP model. In terms of the modification to wide-band B-V color, BSS correction on the SSP model can be quantified.

5.1.   B-V color versus Age

The integrated color of a theoretical SSP changes with time when massive stars leave the blue and luminous MS. Here, the most intuitionistic trend in the picture of conventional SSP model is that the color becomes redder. However, the common existence of BSSs will put a different signature on this scenario. In our work, the 'observed' B-V color with BSSs effects is quite bluer than that predicted by the conventional SSP model. Figure 16 depicts such a modification. Theoretical B-V color of four different metallicities is given in four lines in different types, obtained by convolving the conventional ISEDs made with standard SSP model (assuming Salpeter IMF and using Padova stellar track library) with corresponding filter responses. The solid circles are B-V color (derived with the combined ISEDs) of the twenty-seven sample clusters involving BSSs contribution. It is clearly shown that the B-V color has been dramatically modified by BSSs. All the solid circles lie below the theoretical value of Z=0.02, although 40% of the sample clusters are metal-rich (Z > 0.02). Three lowest points in Figure 16 are those BSS-dominating clusters. As discussed in Section 4, quantitative analysis of BSSs effects on this kind of clusters should be supported by further studies both in observation and theory. Detailed results are listed in Table 2. Columns 1-3 give the name, age, and metallicity of the cluster (age and metallicity parameters follow the same sources as in Table 1). Column 4 is N_2 number. Column 5 is the original BSSs number listed in AL95, while column 6 is the adopted BSSs number in our work (eliminating the BSSs below ZAMS). Finally, columns 7-8 are B-V color resulted from the conventional SSP model and from the BSS-corrected model, respectively.

Assuming that all the sample clusters have solar metallicity (Z=0.02), Figure 17 shows quantitatively the age underestimation when fitting the photometric data with conventional SSP model. The solid line in Figure 17 is theoretical B-V color of Z=0.02 against the age of our sample clusters. Keeping B-V color while doubling the age we get the dash line, and triple the age we get the dotted line. In Figure 17, the smallest deviated points in color can

be approximated with 30% age-expanding conventional SSP model (long-dash line), and the double-age dash line runs through many of the BSS-corrected solid circles.

5.2. B-V color versus Metallicity

As described in Section 2, there is a non-negligible metallicity dispersion in our sample clusters. More than a half of them are metal-poor (Z < 0.02). Since metallicity is an essential parameter for evolution of both stars and galaxies, it will inevitably influence the intrinsic properties of BSSs, therefore brings changes on the BSSs effects on conventional SSP model.

In this work, the possible impact of metallicity on BSSs contribution is detected with the corrected B-V colors as a function of cluster metallicities. Corresponding details are pointed out in Figure 18, where the ordinate is the ratio of B-V alternations caused by BSS component in a cluster to the theoretical B-V color of conventional SSP model, or named relative alternations, and the abscissa is the metallicity of our sample clusters. It seems from Figure 18 that cluster metallicity and BSS contribution are well correlated in the metal-poor case. This is simply stressed in Figure 19 with four typical Z values (Z $\leq$ 0.02), each of which has not less than three samples in this work. In Figure 19, the relative alternations in B-V color increases with metallicity. However, such a correlation does not show in the case of Z > 0.02. We need a complete working sample for this analysis.

5.3. Fitting the ISEDs of open clusters with conventional SSP model: uncertainties

Based on the expatiation in above paragraphs, conventional SSP model derived from the single star evolution theory has been dramatically altered by BSS component in a population. This modification typically enhances the UV and blue parts of the ISEDs, therefore the B-V color of SSPs becomes bluer. If it is to derive an age to a population including BSSs by fitting a conventional SSP model, a substantial uncertainty will be there. Such a conclusion can be visualized by direct fitting the real ISED of a population with the conventional SSP model with depressed either age or metallicity, since both factors make the ISED bluer as the BSS components do as in the case of our sample clusters. In other words, ignoring the existence of BSSs in stellar populations of metallicity and age ranges covered by our sample may seriously under-estimate either age or metallicity of the population by the conventional SSP model.

In this work, the composite ISEDs of open clusters including BSSs contribution are

fitted with the conventional SSP model at younger ages or lower metallicities. A quantitative measure of the uncertainties introduced by BSSs in a population can be given in this way.

Taking the most popular old open clusters NGC 188 and NGC 2682 as examples, the results of best fitting are presented in Figures 20 and 21, respectively. The abscissa is the wavelength in angstrom. The ordinate is the logarithmic value of the absolute flux of ISED normalized at wavelength of 5500 $\mathring{A}$. In the lower parts in figures, the difference between the composite ISED of the cluster and the best-fitting conventional SSP ISED is given as δ, together with the standard deviation σ in the region of $\pm 3\sigma$ in dotted lines. In each figure, the left panel is the fitted result that keeps the same metallicity but younger age, while the right panel is that just the opposite, keeping the same age but lower metallicity. The composite ISED of the cluster is plotted in solid line, the conventional ISED is given in dash line. As a comparison, the basic parameters of the cluster adopted in our work are given in the top right corner in each plot. The parameters of the fitted conventional ISED is given just below the fitting line.

As shown in Figures 20 and 21, conventional SSP model can fit perfectly most of the features of the composite ISED of the cluster, if we let the age or metallicity free. The exception is at the extreme UV part of the SED. As we can see from the best fitting parameters, both age and metallicity can change by a factor of 2 in our examples.

6. SUMMARY AND DISCUSSIONS

Aimed at detecting BSSs effects on the integrated properties of conventional SSP model, twenty-seven Galactic open clusters older than 1Gyr and their BSS contents are studied in this work. In general, the ISEDs of our sample clusters have been dramatically modified, and such modification is emphasized in UV and blue bands; In terms of photometry, the integrated B-V color of the sample clusters becomes bluer, this leads to an under-estimation either in age or in metallicity when fitting the observed colors of a target unresolved population with that of a conventional SSP model. The present results are summarized and discussed in the following,

1. In this work, twenty-seven Galactic open clusters older than 1Gyr are selected as our working sample. The photometric data of BSSs including B-V colors and V-band magnitudes, N_{BS} and N_2 number are directly quoted from AL95. The basic parameters of sample clusters from recent literatures are used when they are available.

2. We scheme a semi-empirical approach of building cluster ISED. The general stellar ingredients including all member stars well fitted by a theoretical isochrone are repre-

sented by the conventional SSP model. BSSs are treated as hydrogen-burning MS stars. Their positions in the CMD are fitted with evolutionary tracks of masses higher than the turnoff. Then, a theoretical stellar spectrum is assigned to each BSS, according to parameters (T_{eff} and $log\ g$) derived from the best fitting. Finally, the combination of these two components constructs the modified ISED of the cluster.

3. We have divided the BSSs modifications to conventional ISEDs into three cases, namely, normal star dominate (Fig. 4a), BSSs important (Fig. 4b) and BSSs dominate (Fig. 4c). The modifications are mainly related to the BSSs richness in the clusters and their positions in the observed CMDs. For the first case, BSSs generally locate near the cluster turnoff in the CMD, and the number of BSSs is small when compared with turnoff region stars, therefore they can not produce obvious contribution to the ISED of the cluster. For the second case, BSSs effects get enhanced generally due to: (a). there is a large number of bright BSSs in the cluster; (b). The N_{BS} is small, but there is a few (even just 1!) BSSs which are much brighter than the cluster turnoff point; and (c). the cluster is very member-poor. The third case is an excessive situation. There is at least one extremely luminous BSS in the cluster and/or the cluster is extremely poorly populated. The bright star(s) is so bright that controls almost all the integrated light of the cluster.

4. We have depicted the alternation of B-V color of our sample clusters caused by BSSs. As shown in Figure 16, the B-V color becomes significantly bluer.

5. We have discussed the effects of metallicity on BSSs contribution. As shown in Figure 18, they are well correlated in the metal-poor case (Z < 0.02). In Figure 19, the ratio of the alternation of B-V color increases with metallicity increasing. But the correlation does not follow the case of Z > 0.02.

6. We have scaled the age underestimation of a cluster by fitting the observed B-V color with conventional SSP model. Based on the assumption that all the sample clusters have solar metallicity (Z=0.02), we have shown in Figure 17 that the age of an observed stellar population is seriously under-estimated by conventional SSP model. As clearly shown in Figure 17, 30% uncertainties in ages can be given for the least affected clusters, and for many cases, such corrections amounts to twice of the conventional age.

7. We have also detected the age and metallicity uncertainties when fitting the observed cluster ISED with conventional SSP model, since decreasing either age or metallicity will also make the ISED bluer as inclusion of BSSs does. Taking old open cluster NGC 188 and NGC 2682 as examples, the results of the best fitting show that conventional SSP model can fit perfectly most of the features of the composite ISEDs including

BSSs contribution if we let the age or metallicity free, and both age and metallicity can change by a factor of 2.

8. The modification due to BSSs to the theoretical SSP model corresponding to each cluster show that BSS population is very important, and can be crucial for stellar population analysis of complex stellar system. This is especially true when applying the current EPS technique to unresolved stellar systems. Considering open clusters as typical descendants of regular star forming activities, and regulating our results to the age and metallicity ranges covered by present data set, SSP model derived from single star evolution theory is seriously altered. Therefore, the contribution of such a component should be considered when applying EPS method to more complicated stellar systems.

The present results rely on the photometry from different sources, and the formation mechanisms and the specific properties of BSSs in each cluster vary greatly among the sample, therefore we are limited to draw our conclusion on a single cluster base. With careful cluster physical parameter measurements and membership analysis of individual BSSs, the current results are still meaningful and can be regarded as reference for further investigation on this problem. To reveal the effects of BSSs on stellar populations in all different cases of age, metallicity and environment, systematic observations together with simulations of stellar dynamical processes at all conditions are needed.

REFERENCES

Ahumada, J., & Lapasset, E. 1995, A&AS, 109, 375 (AL95)

Anthony-Twarog, B. J., Mukherjee, K., Twarog, B. A., & Caldwell, N. 1988, AJ, 95, 1453

Anthony-Twarog, B. J., Twarog, B. A., Kaluzny, J., & Shara, M. M. 1990, AJ, 99, 1504

Anthony-Twarog, B. J., Twarog, B. A., Heim, E. A., & Caldwell, N. 1991, AJ, 102, 1056

Aparicio, A., Bertelli, G., Chiosi, C., & Garcia-Pelayo, J. M. 1990, A&A, 240, 262

Aparicio, A., Bertelli, G., Chiosi, C., & Garcia-pelayo, J. M. 1991, A&AS, 88, 155

Arp, H., & Cuffey, J. 1962, ApJ, 136, 51

Bacon, D., Sigurdsson, S., & Davies, M. B. 1996, MNRAS, 281, 830

Bailyn, C. D. 1995, ARA&A, 33, 133

Battinelli, P., Brandimarti, A., & Capuzzo-Dolcetta, R. 1994, A&AS, 104, 379

Benz, W., & Hills, J. G. 1987, ApJ, 323, 614

Benz, W., & Hills, J. G. 1992, ApJ, 389, 546

Bergbusch, P. A., Vandenberg, D. A., & Infante, L. 1991, AJ, 101, 2102

Bertelli, G., Bressan, A., Chiosi, C., Fagotto, F., & Nasi, E. 1994, A&AS, 106, 275

Bica, E., & Alloin, D. 1986, A&AS, 66, 171

Bouchet, P., & The, P. S. 1983, PASP, 95, 474

Boyle, R. P., Kazlauskas, A., Vansevicius, V., Straizys, V., Vrba, F. J., Sudzius, J., & Smriglio, F. 1998, BaltA, 7, 369

Bragaglia, A., Carretta, E., Gratton, R. G., Tosi, M., Bonanno, G., Bruno, P., Calì, A., Claudi, R., Cosentino, R., Desidera, S., and 3 coauthors 2001, AJ, 121, 327

Bressan, A., Chiosi, C., & Fagotto, F. 1994, ApJS, 94, 63

Brown, J. A., Wallerstein, G., Geisler, D., & Oke, J. B. 1996, AJ, 112, 1551

Cannon, R. D., & Lloyd, C. 1969, MNRAS, 144, 449

Canterna, R., Geisler, D., Harris, H. C., Olszewski, E., & Schommer, R. 1986, AJ, 92, 79

Carraro, G., Barbon, R., & Boschetti, C. S. 2002, MNRAS, 336, 259

Carraro, G., & Patat, F. 1995, MNRAS, 276, 563

Chiu, L.-T. G., & van Altena, W. F. 1981, ApJ, 243, 827

Christian, C. A. 1980, AJ, 85, 700

Christian, C. A. 1984, ApJ, 286, 552

Crinklaw, G., & Talbert, F. D. 1991, PASP, 103, 536

Daniel, S. A., Latham, D. W., Mathieu, R. D., & Twarog, B. A. 1994, PASP, 106, 281

Deng, L., Chen, R., Liu, X. S., & Chen, J. S. 1999, ApJ, 524, 824

Dias, W. S., Alessi, B. S., Moitinho, A., & Lépine, J. R. D. 2002, A&A, 389, 871

Dinescu, D. I., Girard, T. M., van Altena, W. F., Yang, T.-G., & Lee, Y.-W. 1996, AJ, 111, 1205

Eggen, O. J., & Sandage, A. R. 1969, ApJ, 158, 669

Eggen, O. J. 1969, ApJ, 155, 439

Eggen, O. J. 1983, AJ, 88, 813

Ferraro, F. R., Paltrinieri, B., Fusi Pecci, F., Cacciari, C., Dorman, B., Rood, R. T., Buonanno, R., Corsi, C. E., Burgarella, D., & Laget, M. 1997, A&A, 324, 915

Ferraro, F. R., Sills, A., Rood, R. T., Paltrinieri, B., & Buonanno, R. 2003, ApJ, 588, 464

Frandsen, S., Dreyer, P., & Kjeldsen, H. 1989, A&A, 215, 287

Friel, E. D., & Janes, K. A. 1993, A&A, 267, 75

Geisler, D. 1988, PASP, 100, 338

Girard, T. M., Grundy, W. M., Lopez, C. E., & van Altena, W. F. 1989, AJ, 98, 227

Gratton, R. G., & Contarini, G. 1994, A&A, 283, 911

Hawarden, T. G. 1976, MNRAS, 174, 471

Hills, J. G., & Day, C. A. 1976, ApL., 17, 87

Kaluzny, J. 1988, AcA, 38, 339

Kaluzny, J. 1989, AcA, 39, 13

Kaluzny, J., & Richtler, T. 1989, AcA, 39, 139

Kaluzny, J., & Rucinski, S. M. 1995, A&AS, 114, 1

Kozhurina-Platais, V., Demarque, P., Platais, I., Orosz, J. A., & Barnes, S. 1997, AJ, 113, 1045

Lejeune, Th., Cuisinier, F., & Buser, R. 1997, A&AS, 125, 229

Lejeune, Th., Cuisinier, F., & Buser, R. 1998, A&AS, 130, 65

Leonard, P. J. T. 1989, AJ, 98, 217

Lindoff, U. 1972, A&AS, 7, 231

Loktin, A. V., Matkin, N. V., & Gerasimenko, T. P. 1994, A&AT, 4, 153

Lombardi, J. C., Jr., Warren, J. S., Rasio, F. A., Sills, A., & Warren, A. R. 2002, ApJ, 568, 939

Manteiga, M., Martinez Roger, C., & Pickles, A. J. 1989, AP&SS, 156, 169

McClure, R. D., Twarog, B. A., & Forrester, W. T. 1981, ApJ, 243, 841

McCrea, W. H. 1964, MNRAS, 128, 147

Paunzen, E., & Maitzen, H. M. 2001, A&A, 373, 153

Pavani, D. B., Bica, E., Dutra, C. M., Dottori, H., Santiago, B. X., Carranza, G., & Díaz, R. J. 2001, A&A, 374, 554

Piersimoni, A., Cassisi, S., Brocato, E., & Straniero, O. 1993, MmSAI, 64, 609

Piotto, G., Zoccali, M., King, I. R., Djorgovski, S. G., Sosin, C., Dorman, B., Rich, R. M., & Meylan, G. 1999, AJ, 117, 264

Pols, O. R., & Marinus, M. 1994, A&A, 288, 475

Richtler, T., & Sagar, R. 2001, BASI, 29, 53

Rosvick, J. M., & Balam, D. 2002, AJ, 124, 2093

Rosvick, J. M., & Vandenberg, D. A. 1998, AJ, 115, 1516

Sandage, A. R. 1953, AJ, 58, 61

Sandage, A. 1962, ApJ, 135, 333

Sanders, W. L. 1977, A&AS, 27, 89

Sanders, W. L. 1989, RMxAA, 17, 31

Sarajedini, A., von Hippel, T., Kozhurina-Platais, V., & Demarque, P. 1999, AJ, 118, 2894

Schiavon, R. P., Caldwell, N., & Rose, J. A. 2004, AJ, 127, 1513

Schönberner, D., & Napiwotzki, R. 1994, A&A, 282, 106

Schulz, J., Fritze-v. Alvensleben, U., Möller, C. S., & Fricke, K. J. 2002, A&A, 392, 1

Stryker, L. L. 1993, PASP, 105, 1081

Turner, D. G. 1983, JRASC, 77, 31

Twarog, B. A., & Anthony-Twarog, B. J. 1995, AJ, 109, 2828

Twarog, B. A., Anthony-Twarog, B. J., & Hawarden, T. G. 1995, PASP, 107, 1215

West, F. R. 1967, ApJS, 14, 384

Wheeler, J. C. 1979, ApJ, 234, 569

Worthey, G., & Jowett, K. J. 2003, PASP, 115, 96

Table 1.　Parameters of the Sample Clusters

ID name	R.A.(2000.0)	Decl(2000.0)	Age(Gyr)	E(B-V)	DM	Z	N_{BS}	N_2	Refe.
Tombaugh 1	07 00 29	-20 34 00	1.0	0.40	13.60	0.02	1	5	(1)
NGC 6208	16 49 28	-53 43 42	1.0^2	0.18^2	10.55^3	0.023^4	5	60	(2) (3) (4)
NGC 2660	08 42 38	-47 12 00	1.2	0.36	12.30	0.02	18	110	(5)
NGC 2158	06 07 25	+24 05 48	1.2	0.55	15.10	0.006	30	150	(6)
NGC 6939	20 31 30	+60 39 42	1.6	0.33	12.27	0.02	4	80	(7)
NGC 3680	11 25 38	-43 14 36	1.6	0.075	10.20	0.026	4	18	(8)
NGC 752	01 57 41	+37 47 06	1.7	0.035	8.25	0.014	1	25	(9)
NGC 2112	05 53 45	+00 24 36	2.0^{10}	0.63^{10}	9.65^{10}	0.014^{11}	15	80	(10) (11)
NGC 7789	23 57 24	+56 42 30	2.0	0.24	12.00	0.016	25	130	(12)
IC 4651	17 24 49	-49 56 00	2.4	0.086	10.10	0.035	8	35	(13)
NGC 6819	19 41 18	+40 11 12	2.5^{14}	0.16^{14}	12.35^{14}	0.025^{15}	33	270	(14) (15)
Berkeley 19	05 24 06	+29 36 00	3.0^{16}	0.40^{16}	13.50^{16}	0.008^{17}	1	10	(16) (17)
NGC 1252	03 10 49	-57 46 00	3.0	0.02	9.04	0.02	1	7	(18)
NGC 2420	07 38 23	+21 34 24	3.4	0.05	11.95	0.007	12	140	(19)
NGC 2506	08 00 01	-10 46 12	3.4	0.05	12.20	0.007	12	130	(20)
NGC 2682	08 51 18	+11 48 00	4.0	0.045	9.38	0.02	30	200	(21)
NGC 7142	21 45 09	+65 46 30	4.5^{22}	0.35^{22}	11.40^{22}	0.016^{23}	23	120	(22) (23)
Melotte 66	07 26 23	-47 40 00	4.5^{24}	0.16^{24}	13.75^{24}	0.008^{25}	46	180	(24) (25)
King 11	23 47 48	+68 38 00	5.0^{26}	1.27^{27}	15.30^{26}	0.012^{27}	24	140	(26) (27)
NGC 2243	06 29 34	-31 17 00	5.0	0.06	13.05	0.007	7	120	(28)
King 2	00 51 00	+58 11 00	6.0^{29}	0.32^{29}	15.20^{26}	0.01^{26}	30	250	(29) (26)
Berkeley 42	19 05 06	+01 53 00	6.0	0.64	10.30	0.012	1	20	(30)
Berkeley 32	06 58 06	+06 26 00	6.3	0.08	12.60	0.012	19	150	(31)
NGC 188	00 47 28	+85 15 18	7.0^{32}	0.09^{32}	11.44^{32}	0.024^{33}	20	170	(32) (33)
NGC 6791	19 20 53	+37 46 18	7.2	0.17	13.52	0.039	27	110	(34)
NGC 1193	03 05 32	+44 23 00	8.0	0.12	13.80	0.01	16	190	(35)
Berkeley 39	07 46 42	-04 36 00	8.0	0.12	13.40	0.01	29	220	(36)

References. — (1): Carraro & Patat 1995, (2): Paunzen & Maitzen 2001, (3): Lindoff 1972, (4): Loktin et al. 1994, (5): Frandsen et al. 1989, (6): Piersimoni et al. 1993, (7): Rosvick & Balam 2002, (8): Kozhurina-Platais et al. 1997, (9): Daniel et al. 1994, (10): Carraro et al. 2002, (11): Brown et al. 1996, (12): Friel & Janes 1993, (13): Anthony-Twarog et al. 1988, (14): Rosvick & Vandenberg 1998, (15): Bragaglia et al. 2001, (16): Christian 1980, (17): Christian 1984, (18): Pavani et al. 2001, (19): Anthony-Twarog et al. 1990, (20): McClure et al. 1981, (21): Boyle et al. 1998, (22): Crinklaw & Talbert 1991, (23): Canterna et al. 1986, (24): Twarog et al. 1995, (25): Gratton & Contarini 1994, (26): Kaluzny 1989, (27): Dias et al. 2002, (28): Bergbusch et al. 1991, (29): Aparicio et al. 1990, (30): Aparicio et al. 1991, (31): Richtler & Sagar 2001, (32): Sarajedini et al. 1999, (33): Worthey & Jowett 2003, (34): Kaluzny & Rucinski 1995, (35): Kaluzny 1988, (36): Kaluzny & Richtler 1989

Table 2.   Color Modifications of the Clusters

ID name	Age(Gyr)	Z	N_2	$N_{BS}{}^O$	$N_{BS}{}^A$	$(B\text{-}V)_{iso}$	$(B\text{-}V)_{iso+BSs}$
Tombaugh 1	1.0	0.02	5	1	1	0.285	0.615
NGC 6208	1.0	0.023	60	5	3	0.596	0.626
NGC 2158	1.2	0.006	150	30	30	0.333	0.519
NGC 2660	1.2	0.02	110	18	18	0.460	0.644
NGC 6939	1.6	0.02	80	4	4	0.474	0.743
NGC 3680	1.6	0.026	18	4	4	0.608	0.752
NGC 752	1.7	0.014	25	1	1	0.671	0.713
NGC 2112	2.0	0.014	80	15	14	0.543	0.756
NGC 7789	2.0	0.016	130	25	24	0.487	0.763
IC 4651	2.4	0.035	35	8	7	0.646	0.856
NGC 6819	2.5	0.025	270	33	32	0.678	0.835
Berkeley 19	3.0	0.008	10	1	1	0.790	0.795
NGC 1252	3.0	0.02	7	1	1	0.263	0.849
NGC 2420	3.4	0.007	140	12	12	0.764	0.771
NGC 2506	3.4	0.007	130	12	11	0.769	0.771
NGC 2682	4.0	0.02	200	30	21	0.762	0.914
Melotte 66	4.5	0.008	180	46	46	0.823	0.823
NGC 7142	4.5	0.016	120	23	22	0.634	0.879
NGC 2243	5.0	0.007	120	7	7	0.802	0.819
King 11	5.0	0.012	140	24	12	0.683	0.858
King 2	6.0	0.01	250	30	30	0.681	0.858
Berkeley 42	6.0	0.012	20	1	1	0.645	0.872
Berkeley 32	6.3	0.012	150	19	18	0.645	0.873
NGC 188	7.0	0.024	170	20	17	0.841	0.960
NGC 6791	7.2	0.039	110	27	18	0.799	1.028
NGC 1193	8.0	0.01	190	16	15	0.777	0.896
Berkeley 39	8.0	0.01	220	29	28	0.749	0.896

[O]The original BSSs number listed in AL95

[A]The BSSs number adopted in our work, eliminating the BSSs below ZAMS
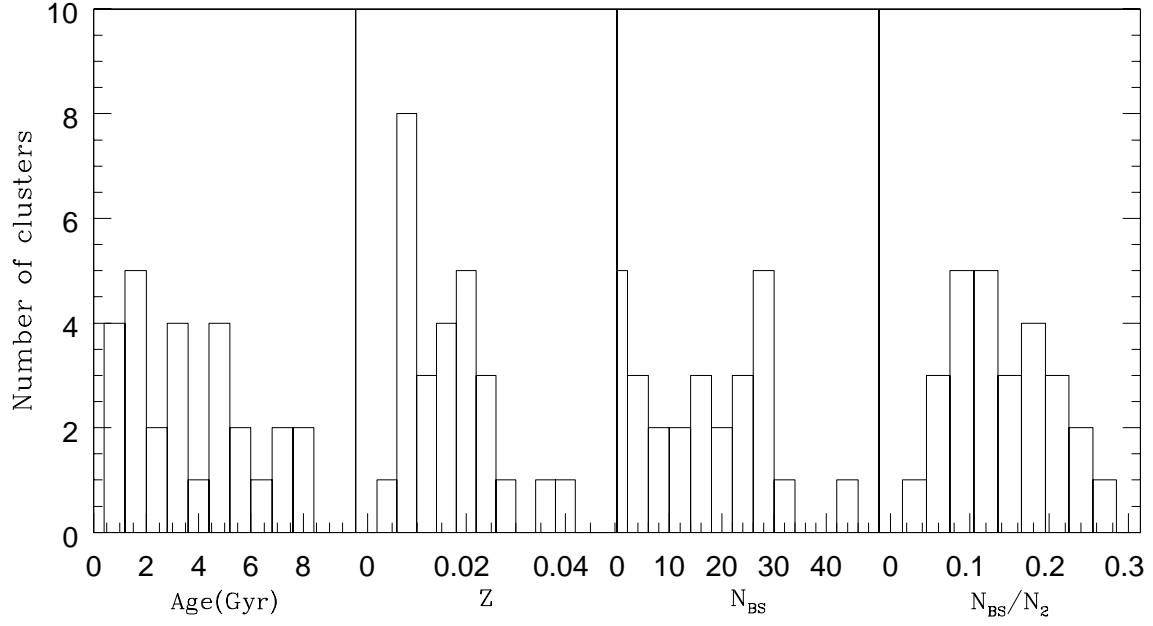
Fig. 1.— Distributions of the open cluster sample according to four different parameters: Age, Z, N_{BS} and N_{BS}/N_2.
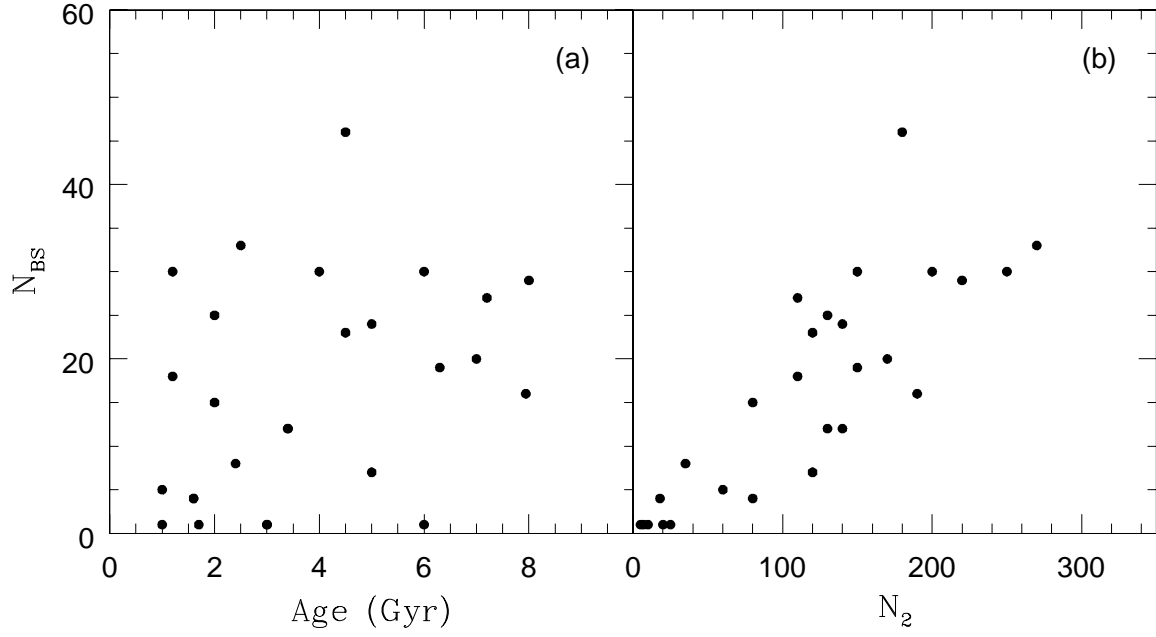
Fig. 2.— (a): Number of BSSs per open cluster in cluster age interval. (b): Number of BSSs per open cluster in N_2 interval.
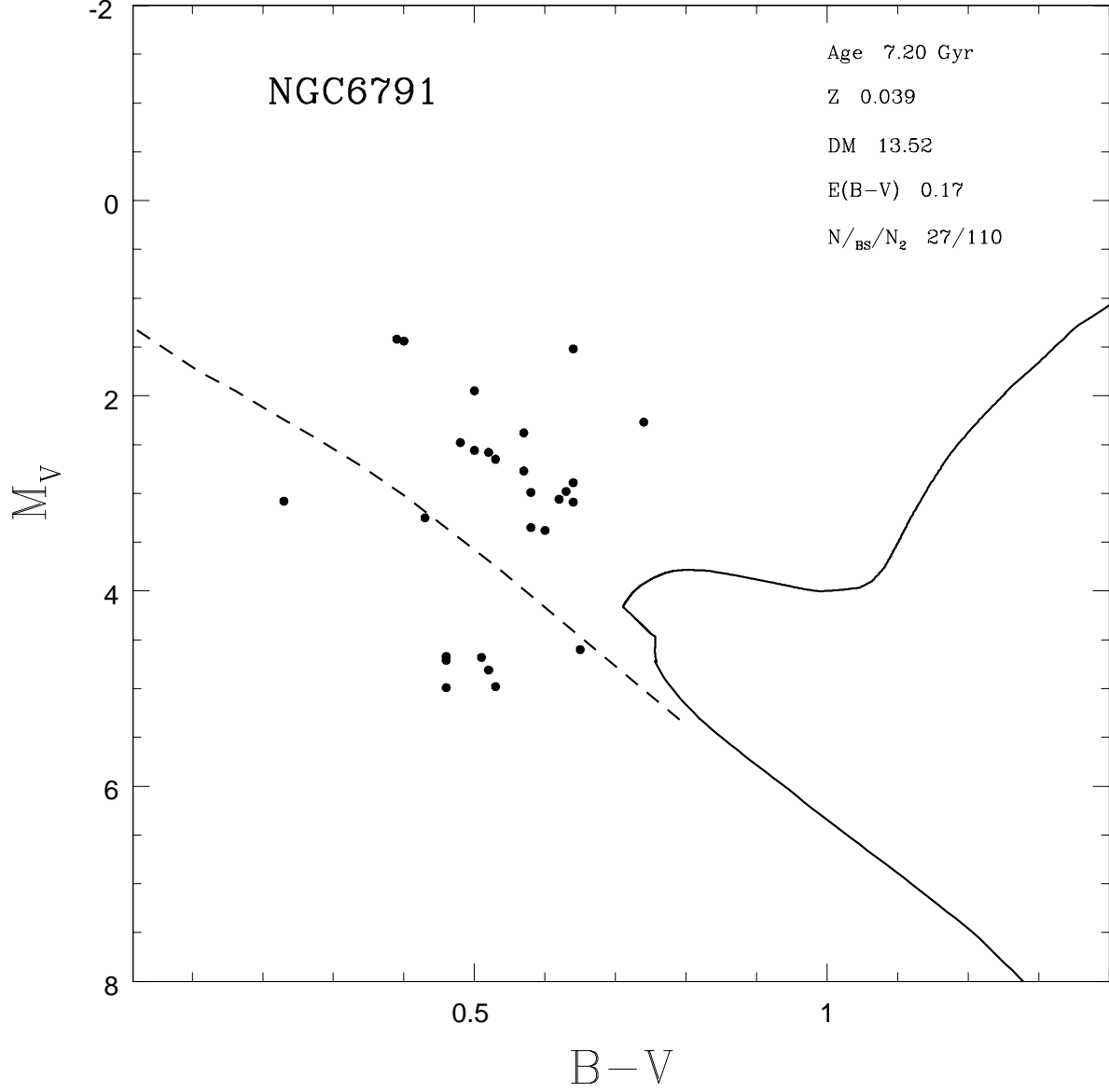
Fig. 3.— The CMD of NGC 6791. *Solid line* : Theoretical isochrone according to the given age (7.2 Gyr) and metallicity (Z=0.039). *Dash line* : ZAMS. *Solid circles* : BSSs.
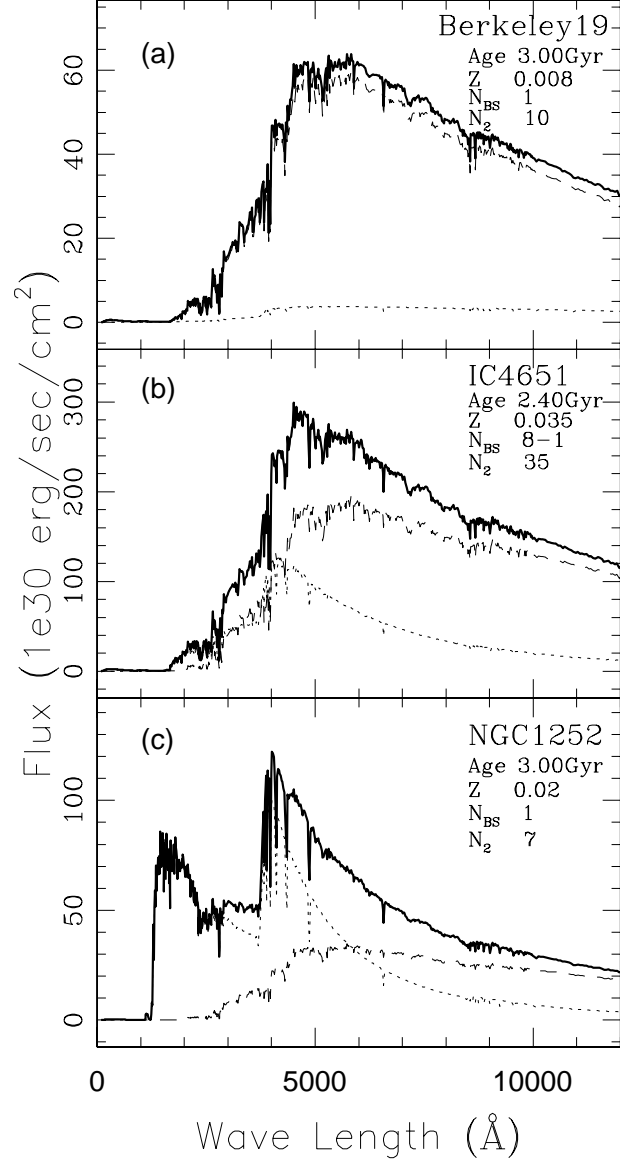
Fig. 4.— The ISEDs modified by BSSs in different degrees. (a): Normal star dominate. (b): BSSs important. (c): BSSs dominate. *Dotted line* : ISED of BSSs only. *Dash line* : ISED of isochrone only. *Solid line* : The composite ISED of isochrone and BSSs.
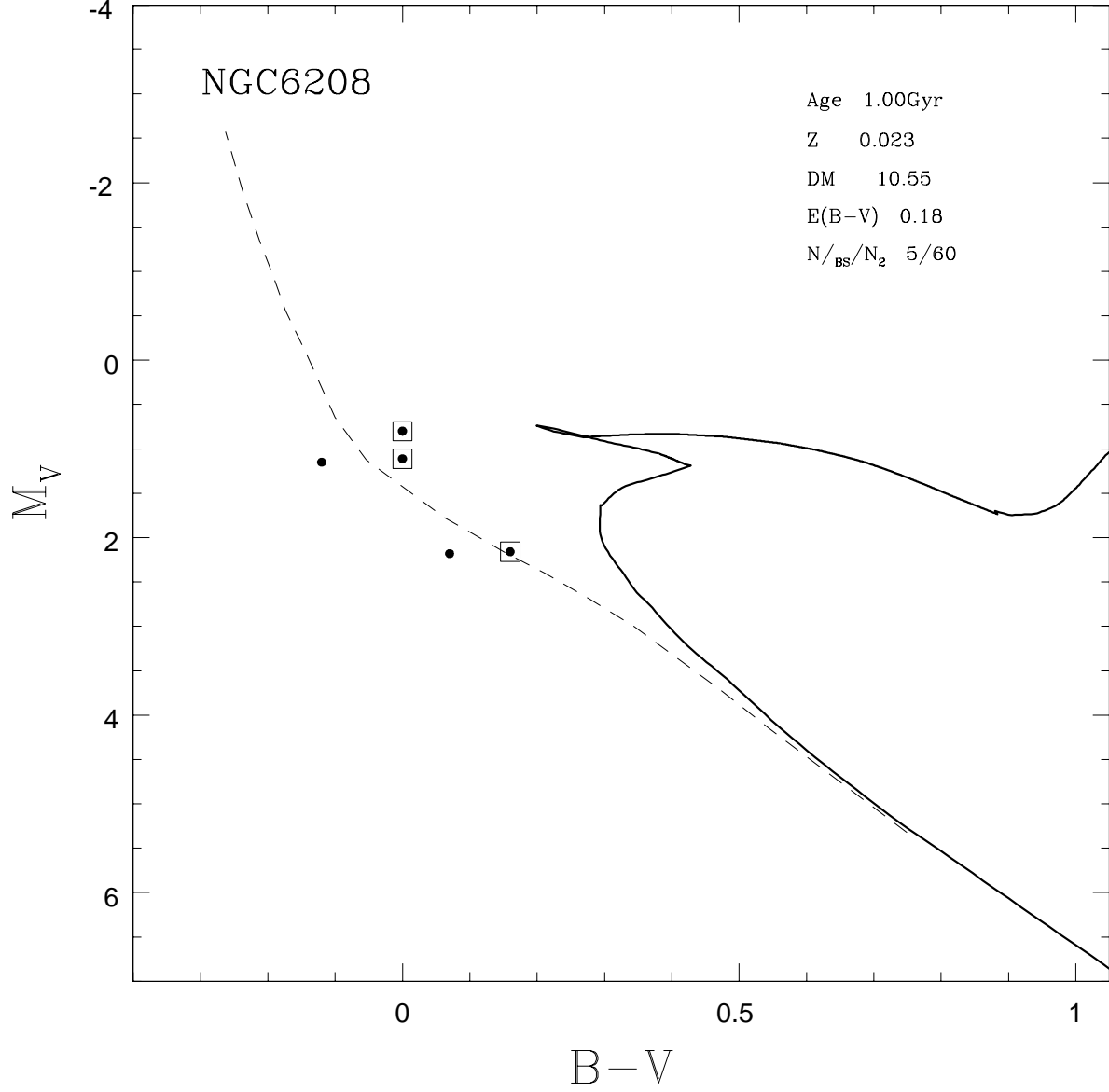
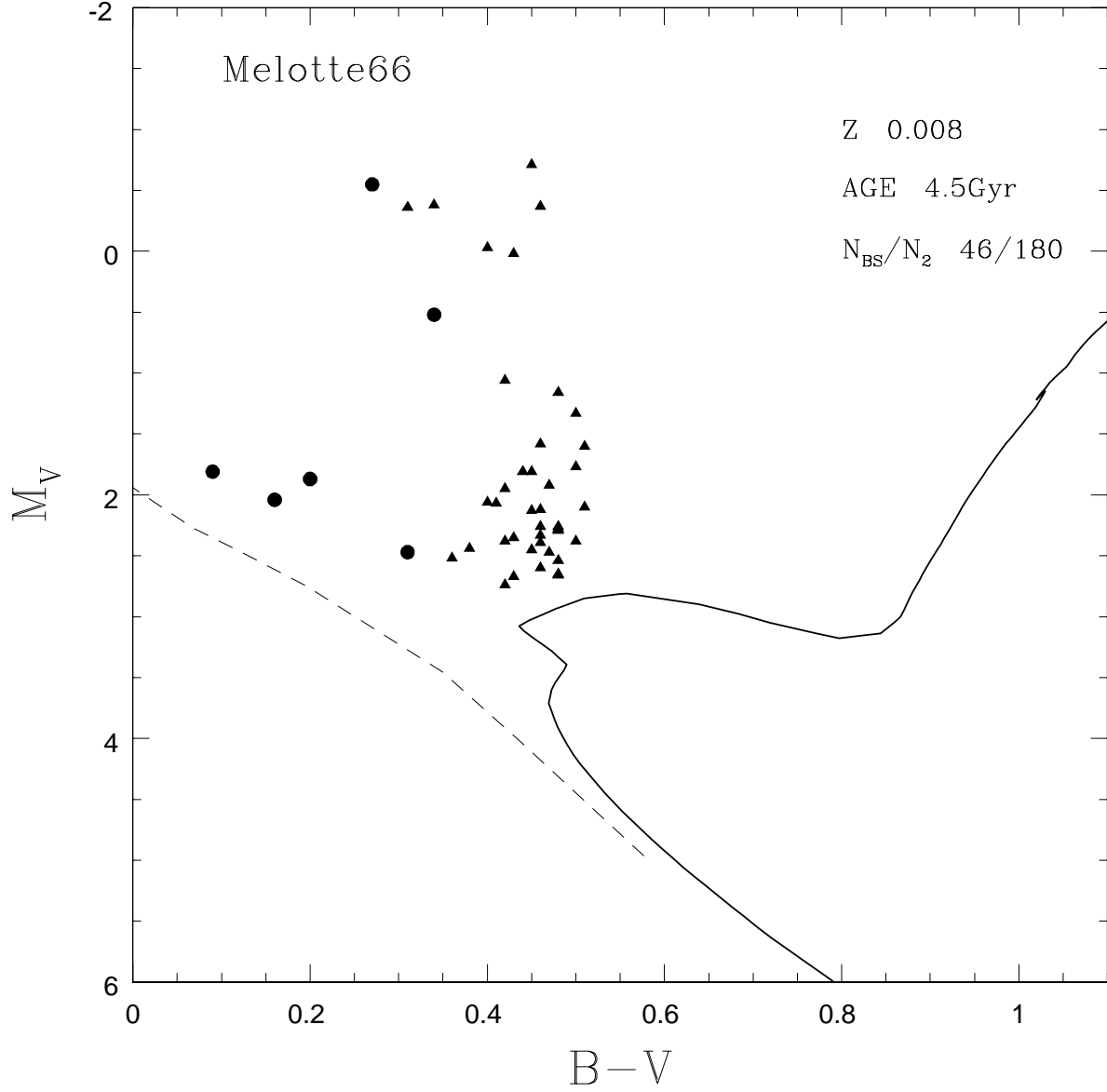Fig. 5.— The CMD of NGC 6208. *Solid line* : Theoretical isochrone. *Dash line* : ZAMS. *Solid triangles* : Five BSSs of NGC 6208 listed in AL95. *Open rectangles* : Three non-member BSSs in Lindoff (1972).
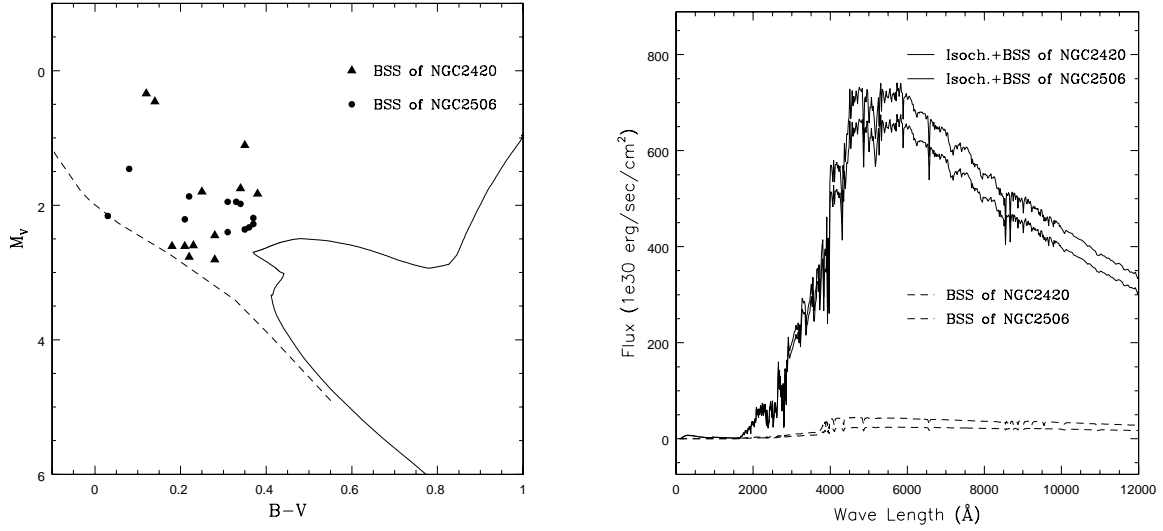
Fig. 6.— A comparison of BSS distributions and ISED modifications between NGC 2420 and NGC 2506. The left panel is the CMD, where the *Solid line* : is the theoretical isochrone with age (3.4 Gyr) and metallicity (Z=0.007), *Dash line* : is the ZAMS, *Solid circles* : are BSSs in NGC 2506, and *Solid triangles* : are BSSs in NGC 2420. In the ISED plot (the right panel), *Thick solid line* : is the ISED of isochrone plus BSSs in NGC 2420, *Thin solid line* : is the ISED of isochrone plus BSSs in NGC 2506, *Thick dash line* : is the ISED of BSSs in NGC 2420, and *Thin dash line* : is the ISED of BSSs in NGC 2506.

King2

Age 6.00 Gyr

Z 0.01

DM 15.20

E(B−V) 0.32

$N/_{BS}N_2$ 30/250

M_V

B−V
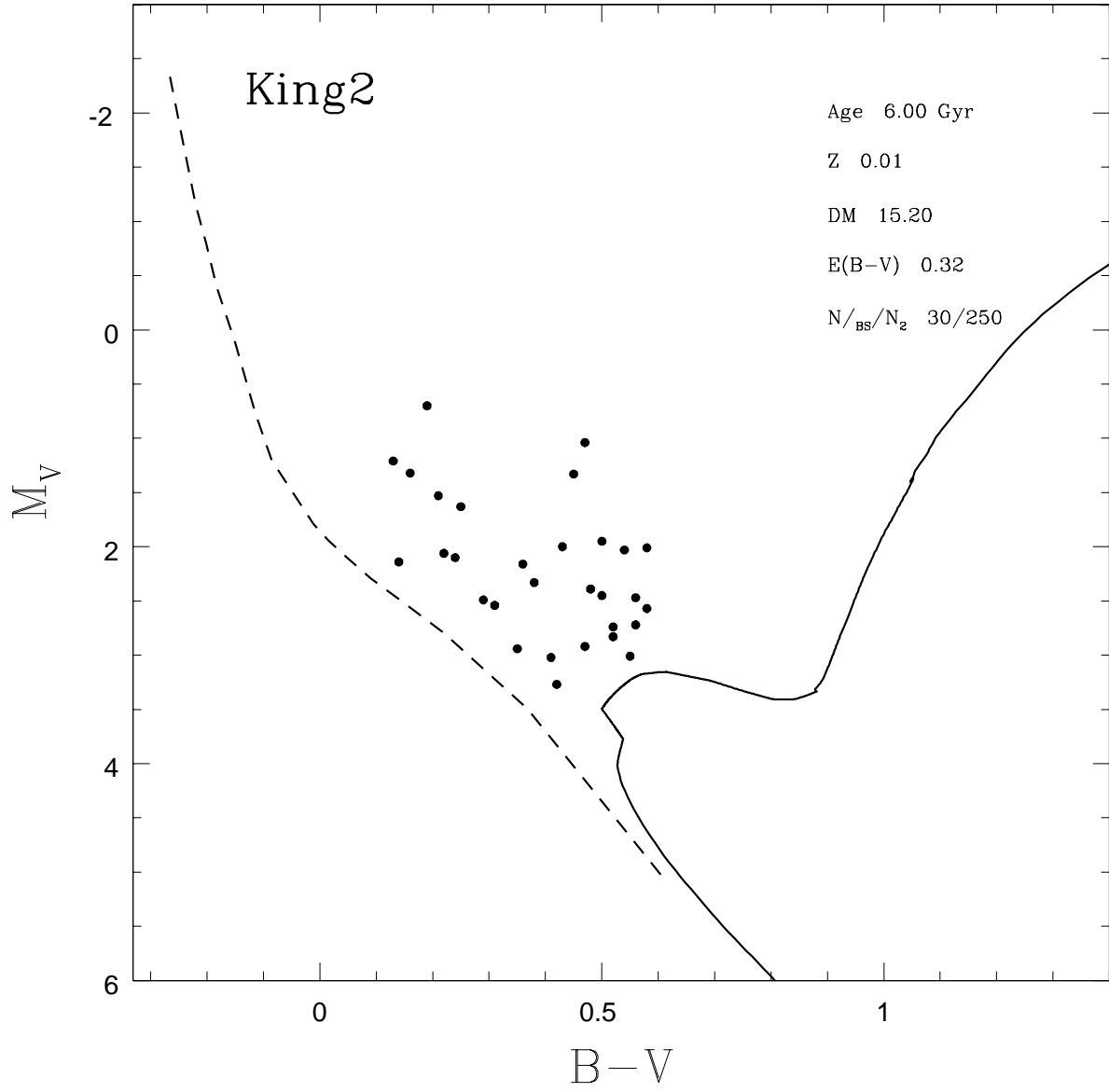
Fig. 7.— The CMD of open cluster King 2.

NGC6939

Age 1.60 Gyr

Z 0.02

DM 12.27

E(B−V) 0.33

N_{BS}/N_2 4/80

M_V

B−V
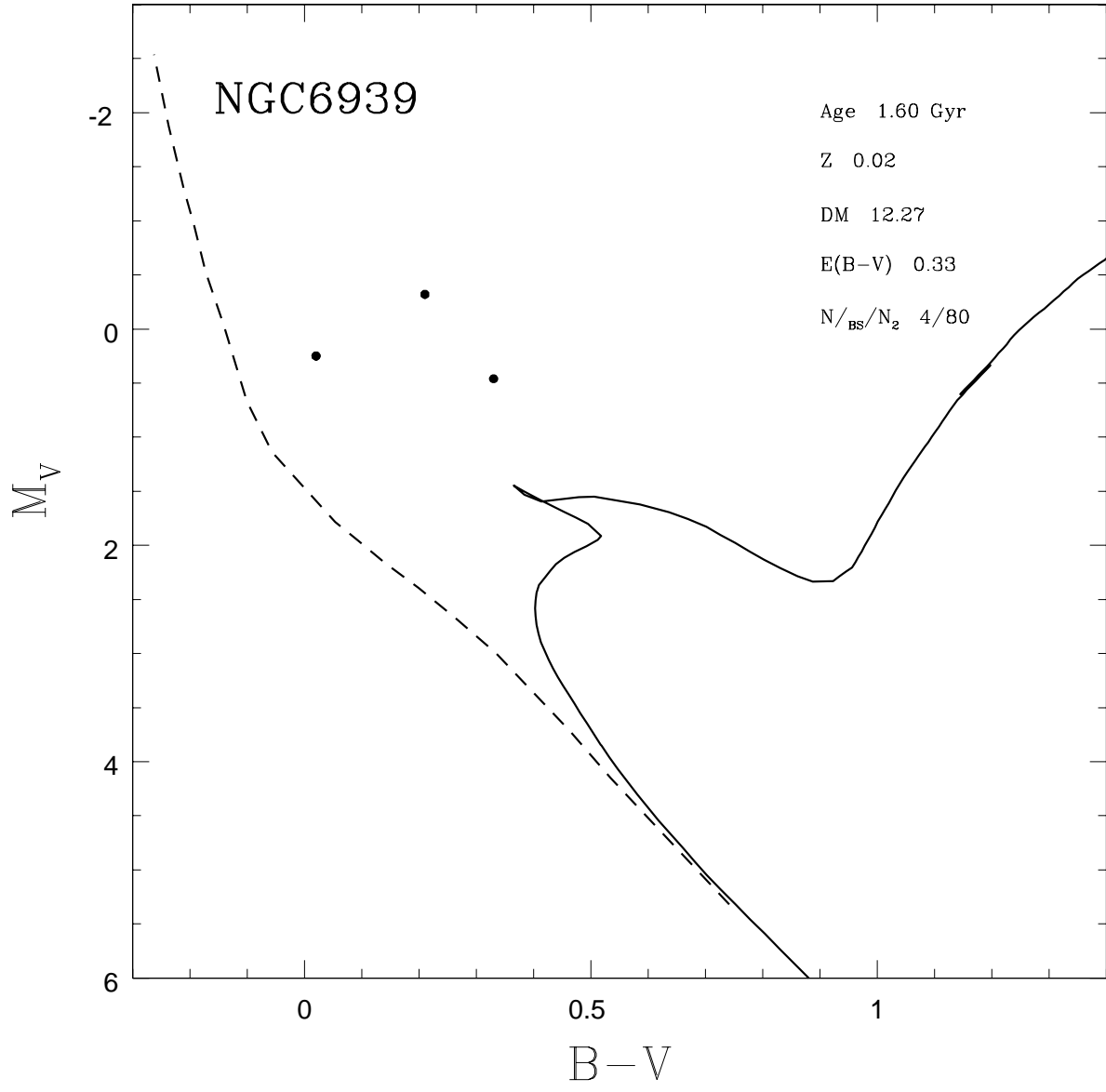
Fig. 8.— The CMD of open cluster NGC 6939.
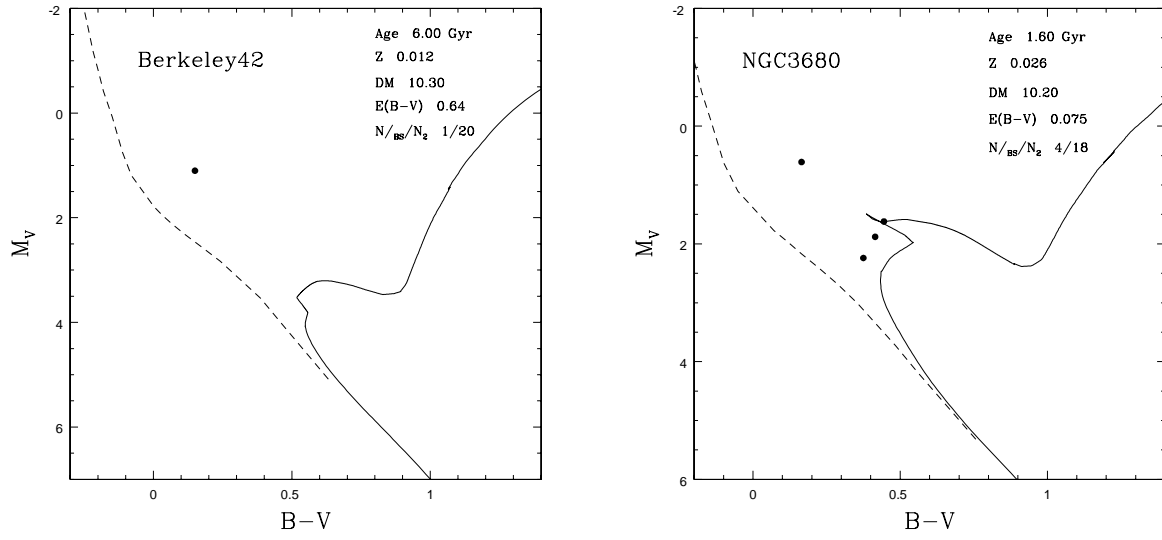
Fig. 9.— CMDs of open cluster Berkeley 42 and NGC 3680.
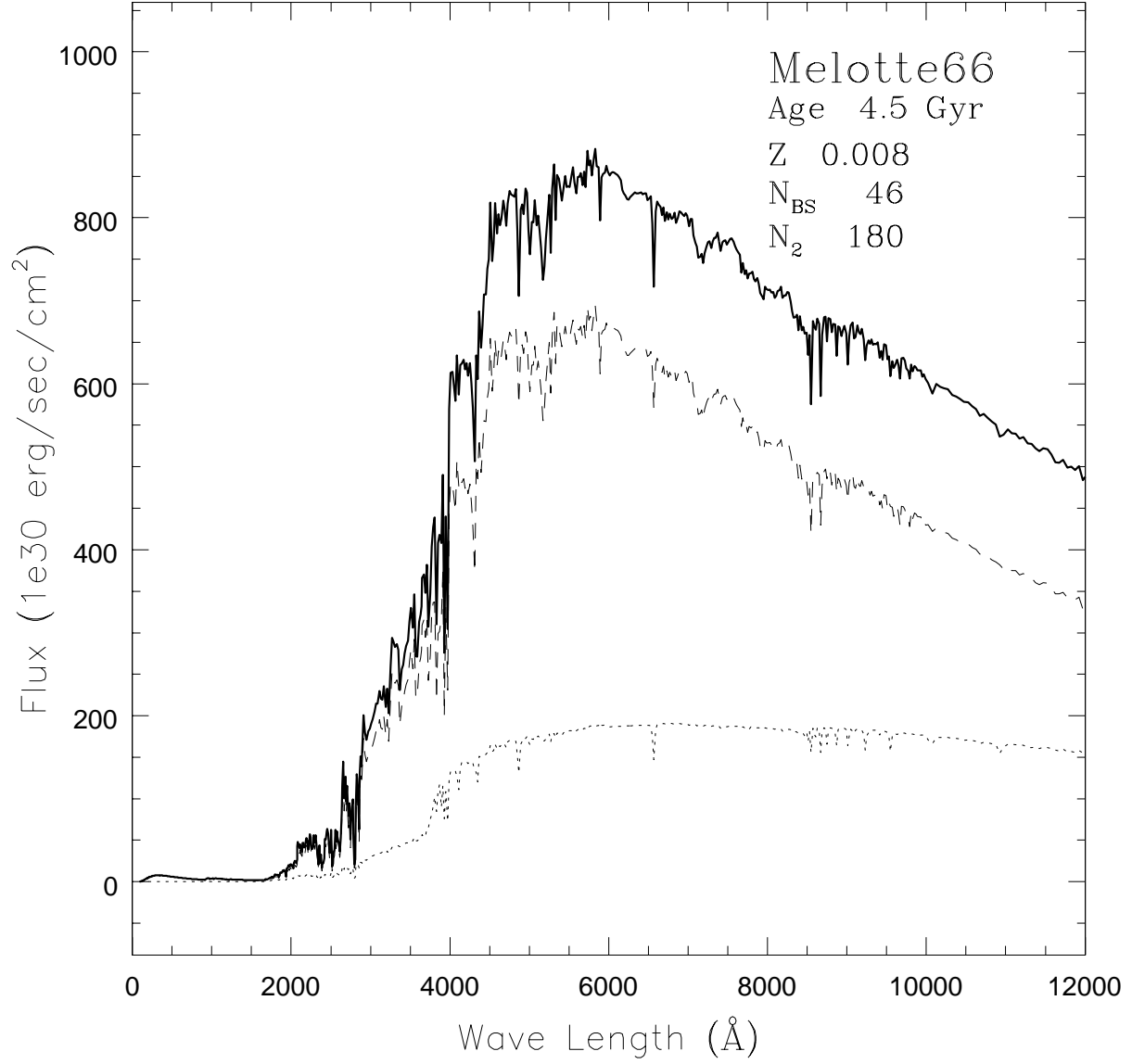
Fig. 10.— The ISED of Melotte 66. *Dotted line* : ISED of BSSs only. *Dash line* : ISED of isochrone only. *Solid line* : The composite ISED of isochrone and BSSs.

Fig. 11.— The CMD of Melotte 66. *Solid line* : Theoretical isochrone according to the given age (8 Gyr) and metallicity (Z=0.008). *Dash line* : ZAMS. *Solid circles* : Six blue-spectrum BSSs in the cluster. *Solid triangles* : Forty red-spectrum BSSs.
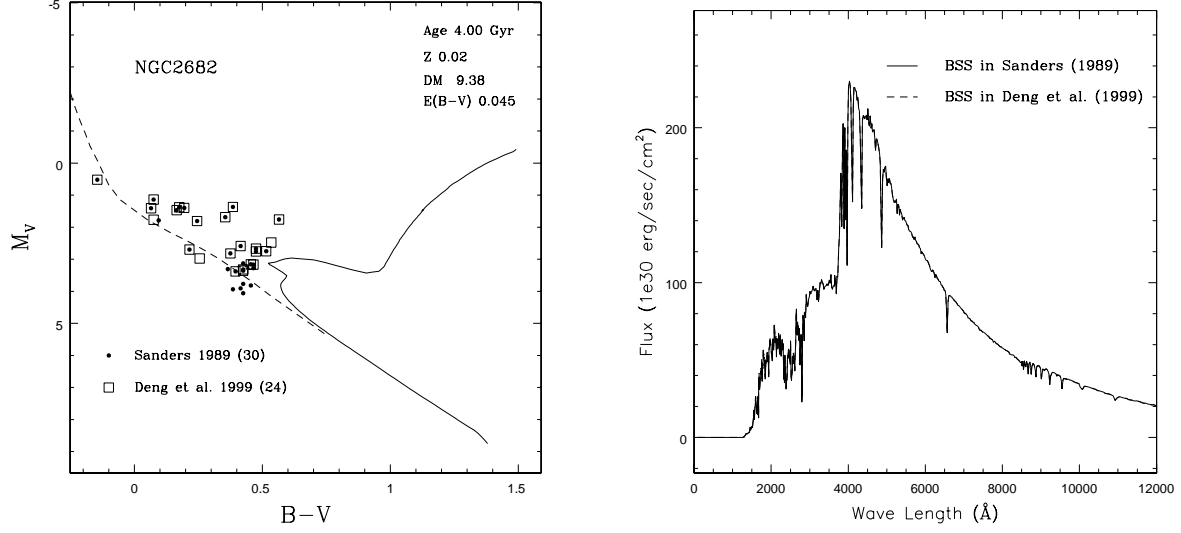
Fig. 12.— Comparison with BSSs identifications in two work of NGC 2682. In the CMD, *solid dots* are BSSs in Sanders (1989), and *open rectangles* are BSSs in Deng et al. (1999). In the ISED, *solid line* is the integrated light of BSSs in Sanders (1989), and *dash line* is that in Deng et al. (1999).
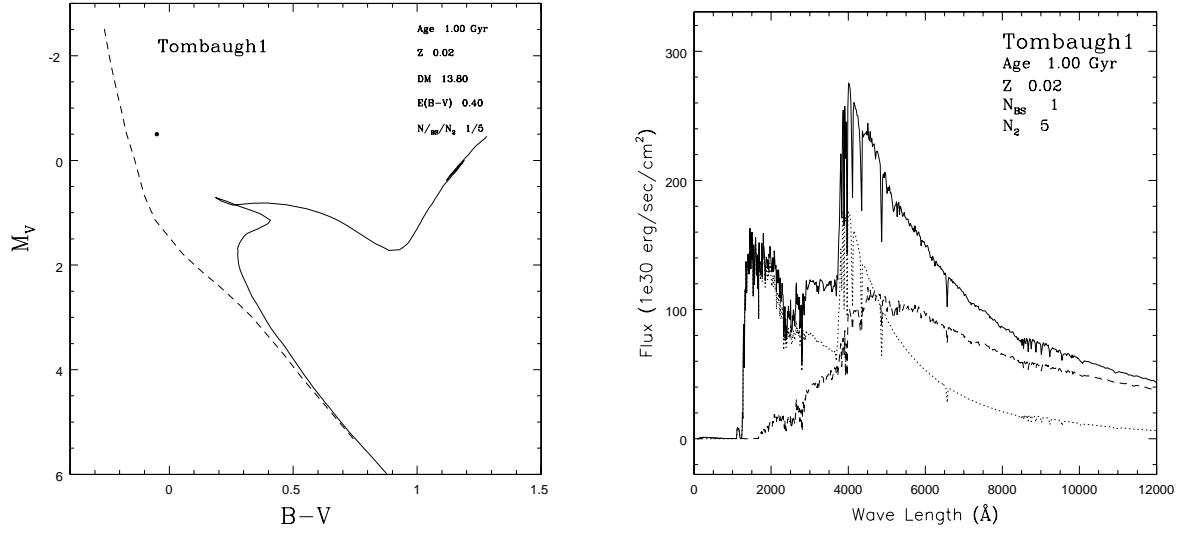
Fig. 13.— The CMD and ISED of Tombaugh 1.
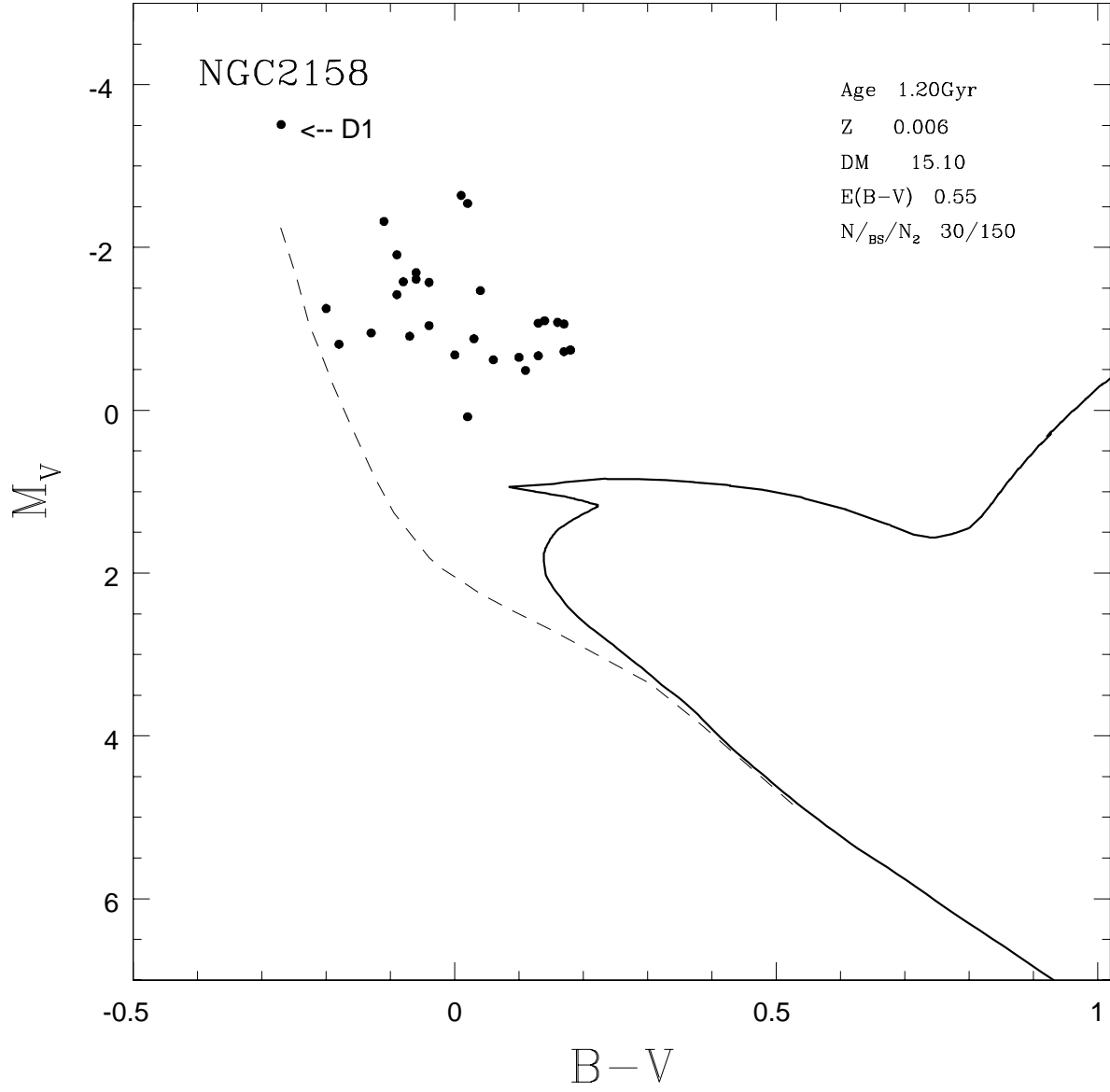
Fig. 14.— The CMD of NGC 2158. *Solid line* : Theoretical isochrone with age (1.2 Gyr) and metallicity (Z=0.008). *Dash line* : ZAMS. *Solid circles* : BSSs. 'D1' is the brightest BSS in the cluster.
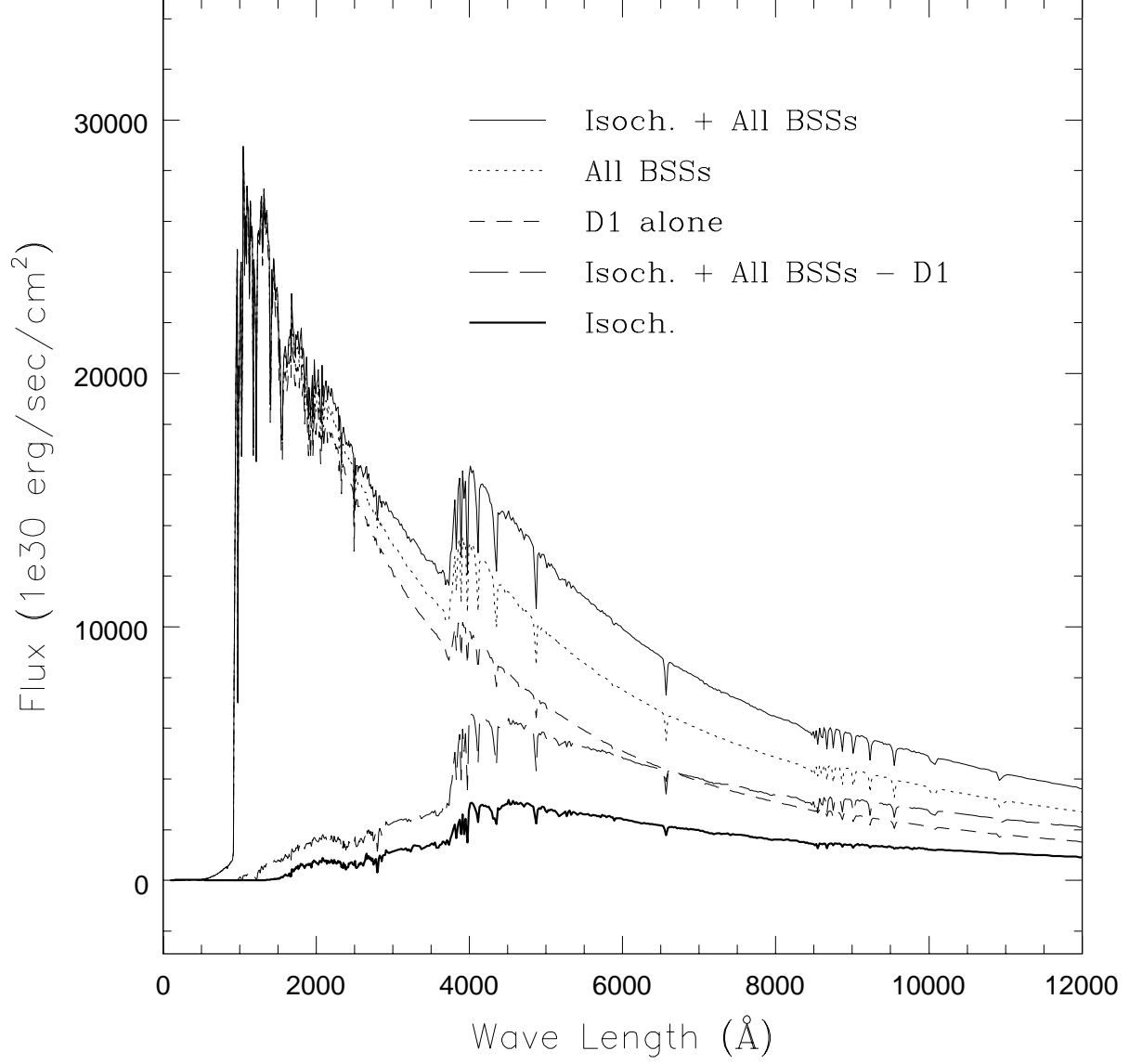
Fig. 15.— Integrated flux of NGC 2158. The contribution of BSSs population is taken apart. *Thick solid line* : ISED of isochrone. *Long dash line* : All components except D1. *Short dash line* : D1 alone. *Thin solid line* : All components (Isochrone and all BSSs).
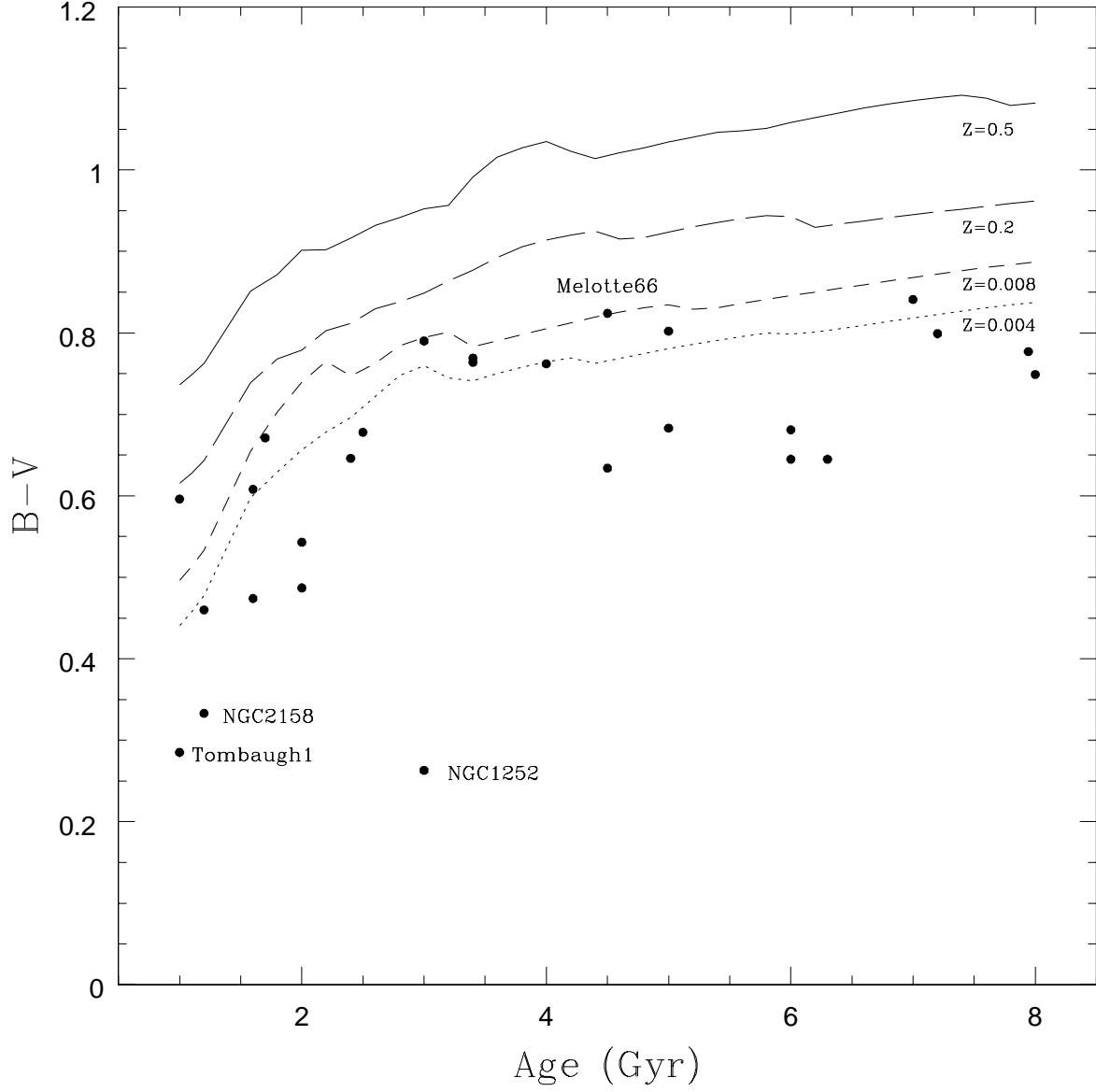
Fig. 16.— B-V color modified by BSSs. Four lines are theoretical values according to different metallicities. The *Solid circles* are B-V color of our sample clusters involving BSSs contribution.
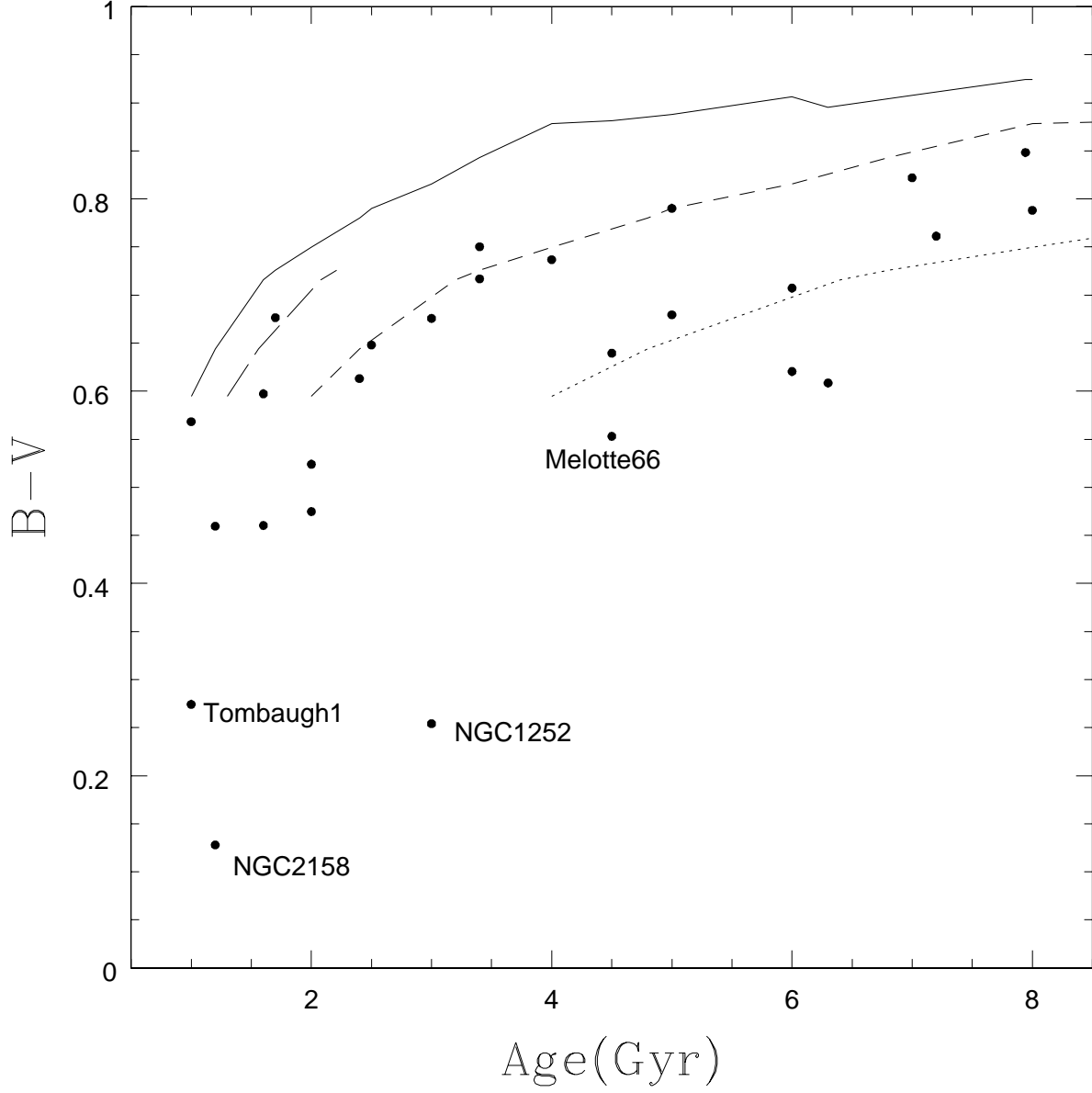
Fig. 17.— Detecting age underestimation of star clusters when fitting the observed color with conventional SSP model. Assuming all the sample clusters with solar metallicity, the *solid line* is theoretical B-V color. Keeping B-V values and double age is the *Dash line*, and triple age is the *dotted line*. The *long dash line* is plotted with age 30%-expanding of the conventional value.
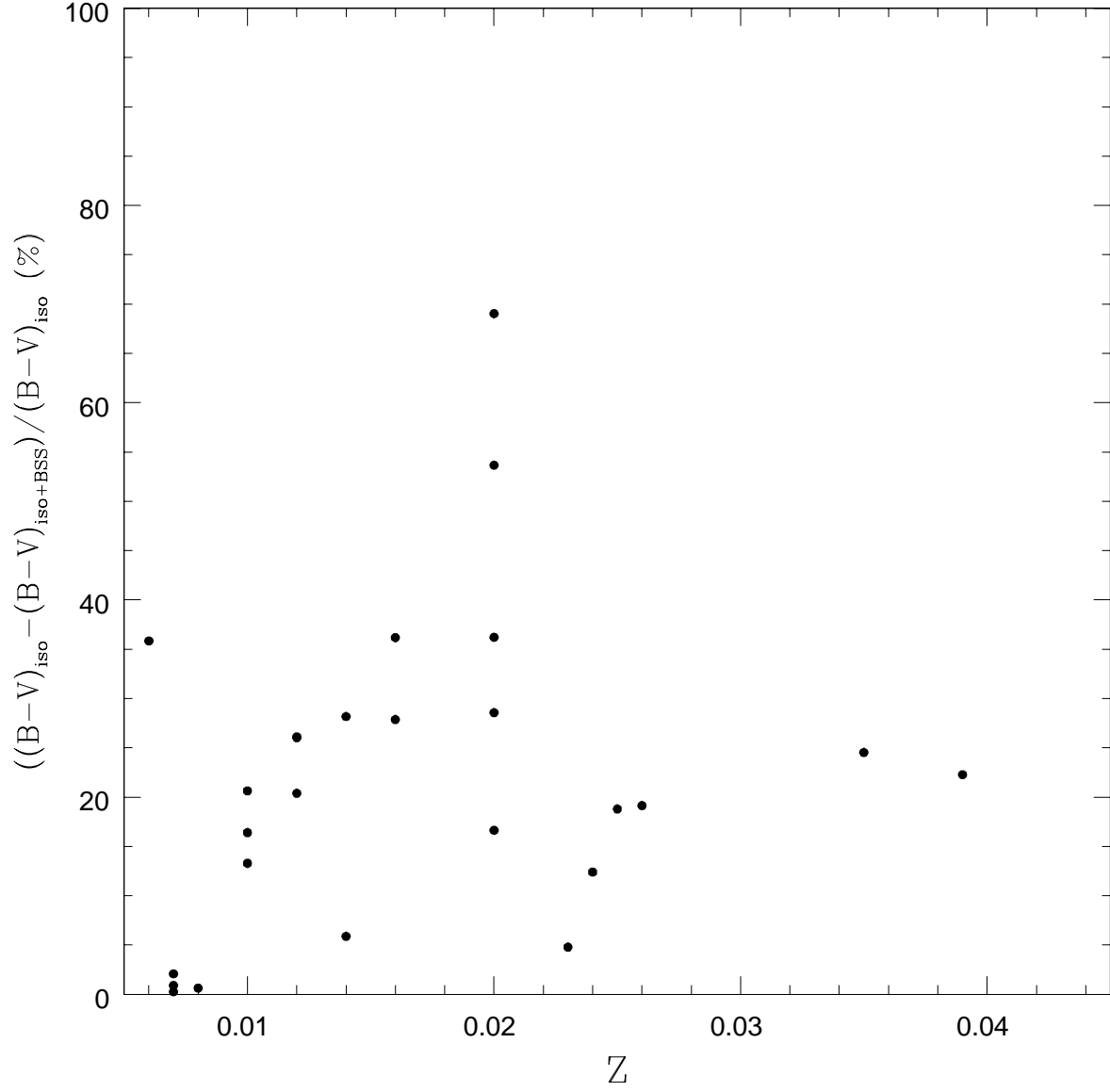
Fig. 18.— Correlation between metallicity and the ratio of the alternation of B-V color caused by BSSs to the conventional B-V color.
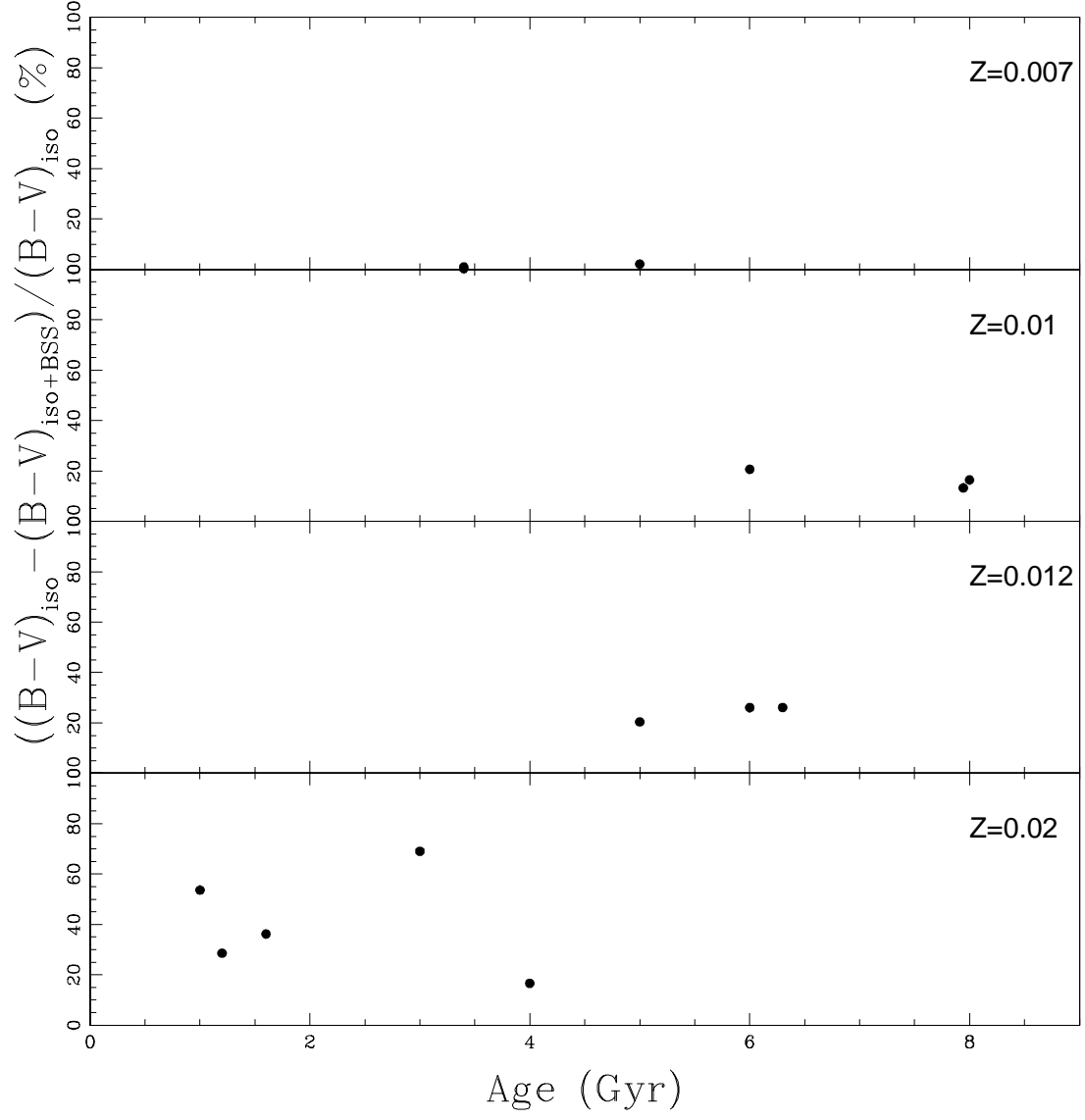
Fig. 19.— BSSs contribution to cluster B-V color, presented with four metallicities: Z=0.007, Z=0.01, Z=0.012 and Z=0.02.
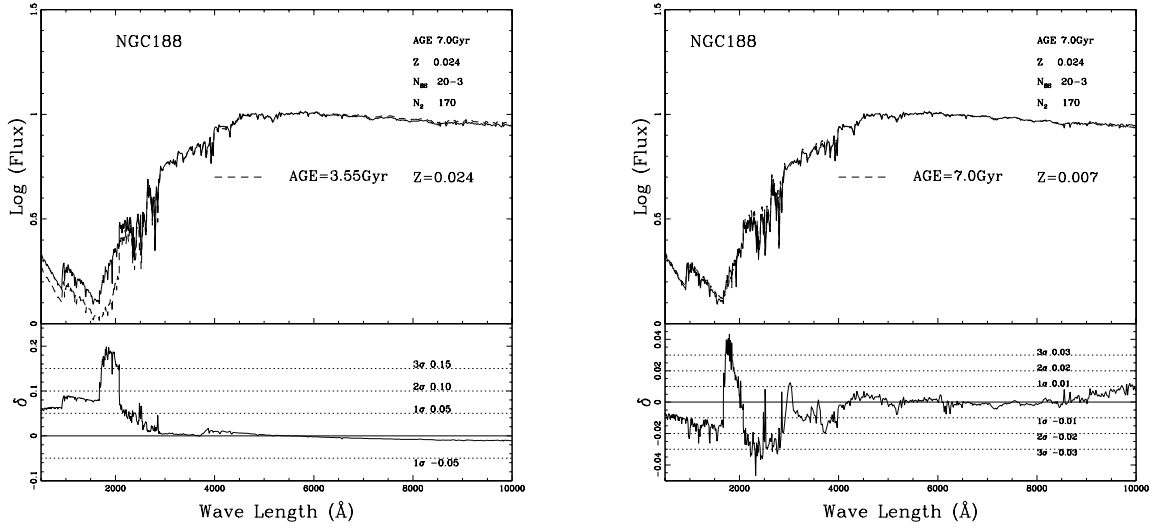
Fig. 20.— Fitting the composite ISED of NGC 188 with conventional SSP model. The abscissa is the wavelength in angstrom. The ordinate is the Log(FLUX), which is the logarithmic value of the absolute flux of the ISED and is normalized at 5500 $\mathring{A}$. δ is the difference between the composite and conventional ISEDs, the direct subtraction of these two fluxes. Standard deviation σ is given in dotted lines in $\pm 3\sigma$. The left panel is the fitting result of keeping the same metallicity but younger age, while the right panel is that just the opposite, keeping the same age but lower metallicity. The composite ISED is plotted in solid line. The conventional ISED is given in dash line. The basic parameters of the cluster adopted in our work are listed in the top right corner in each panel. The parameters of the conventional ISED are given below the fitting line.
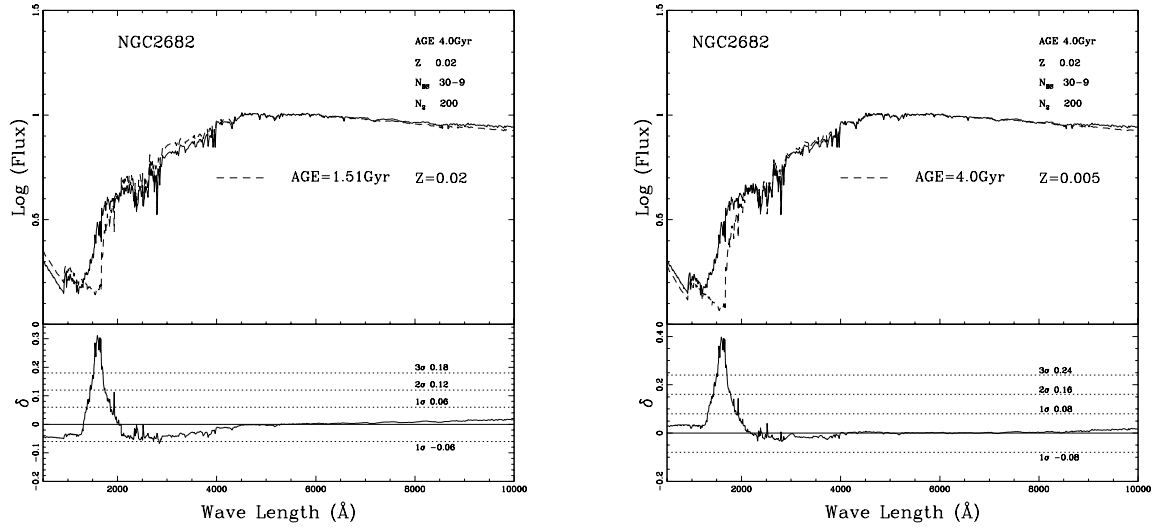
Fig. 21.— Similar to Figure 20, but for NGC 2682.